TITLE: DDX24, a D-E-A-D box RNA helicase, is required for muscle fiber organization and anterior pole specification essential for head regeneration in planarians.

AUTHORS: Souradeep R. Sarkar[1], Vinay Kumar Dubey[2,3], Anusha Jahagirdar[2], Vairavan Lakshmanan[2], Mohamed Mohamed Haroon[2,4], Sai Sowndarya[2], Ramanathan Sowdhamini[1], Dasaradhi Palakodeti[2,5]

AUTHOR AFFILIATIONS:

[1]National Centre for Biological Sciences (NCBS), Tata Institute of Fundamental Research (TIFR), Bengaluru 560065, India.

[2]Integrative Chemical Biology (ICB), Institute for Stem Cell Science and Regenerative Medicine (inStem), Bengaluru 560065, India.

[3]Manipal Academy of Higher Education, Manipal 576104, India.

[4] SASTRA University, Thanjavur 613401, India.

[5]Corresponding author. E-mail id: dasaradhip@instem.res.in

RUNNING TITLE: DDX24 is required for planarian head regeneration.

KEYWORDS: Planaria, Regeneration, Muscle, DEAD Box RNA Helicase, Muscle Fiber Architecture, Anterior Pole, Positional Information, Position Control Genes, Ribosomal RNA.

ABSTRACT: Planarians have a remarkable ability to undergo whole-body regeneration. The timely establishment of polarity at the wound site followed by the specification of the organizing centers- the anterior pole and the posterior pole, are indispensable for successful regeneration. In planarians, polarity, pole, and positional-information determinants are predominantly expressed by muscles. The molecular toolkit that enables this functionality of planarian muscles however remains poorly understood. Here we report that SMED_DDX24, a D-E-A-D Box RNA helicase and the homolog of human DDX24, is critical for planarian head regeneration. DDX24 is enriched in muscles and its knockdown leads to defective muscle-fiber organization and failure to re-specify anterior pole/organizer. Overall, loss of DDX24 manifests into gross misregulation of many well-characterized positional-control genes and patterning-control genes, necessary for organogenesis and tissue positioning and tissue patterning. In addition, wound-induced Wnt signalling was also upregulated in *ddx24* RNAi animals. Canonical WNT-βCATENIN signalling is known to suppress head identity throughout bilateria, including planarians. Modulating this Wnt activity by *β-catenin-1* RNAi, the effector molecule of this pathway, partially rescues the *ddx24* RNAi phenotype, implying that a high Wnt environment in *ddx24* knockdown animals likely impedes their normal head regeneration. Furthermore, at a sub-cellular level, RNA helicases are known to regulate muscle mass and function by regulating their translational landscape. *ddx24* knockdown leads to the downregulation of large subunit ribosomal RNA and the 80S ribosome peak, implying its role in ribosome biogenesis and thereby influencing the translational output. This aspect seems to be an evolutionarily conserved role of DDX24. In summary, our work demonstrates the role of a D-E-A-D box RNA helicase in whole-body regeneration through muscle fiber organization, and pole and positional-information re-specification, likely mediated through translation regulation.

INTRODUCTION

Planarian flatworms have exceptional ability to undergo whole-body regeneration (1,2). Although this observation has fascinated scientists for centuries, the long-standing question of how this is accomplished remains to be completely understood. One critical determinant of planarian regeneration is the timely establishment of regeneration polarity at the wound site. Anterior facing wounds regenerate the head whereas posterior facing wounds regenerate the tail- this is known as regeneration polarity. Anterior polarity, for example, is determined by the expression of the Wnt antagonist *notum* at anterior facing wounds (3). This process is then followed by anterior-pole determination (4–9). The anterior-pole is the Spemann-Mangold organizer equivalent in planarians (10–12). Therefore, precise spatial and temporal determination of this pole is necessary for the head regeneration as well as patterning of different tissues within the head primordia. Further, in the intact animal, constitutive and regional expression of various morphogens and other positional-control genes (PCGs) is necessary for the maintenance of size, shape, and positional identity for different tissues (10,13–19). During regeneration, it becomes necessary to adjust the expression of these PCGs to reset positional information within the existing animal fragment (20–23). Factors regulating PCG expression, critical for the re-establishment of head-trunk-tail identity, remains an active area of investigation.

Planarian muscles, in addition to their canonical roles in locomotion and skeletal support, predominantly express all the positional-control genes and morphogens associated with positional information establishment and patterning (24,25). Furthermore, muscles in planarians also act as ‘structural scaffolds’ for organ regeneration and perform the role of connective tissue by expressing many of the matrisome related genes (26–28). Therefore, given the multi-faceted functional role of muscle in regeneration, defect in muscle organization or loss of muscle associated factors inadvertently leads to defective regeneration (26,29–

32). Molecules and mechanisms that underlie this functional versatility of planarian muscles however remain under-explored.

Post-transcriptional regulatory processes essential for fine-tuning gene expression have gained importance because of their critical role in various cellular functions (33–38). RNA helicases play a central role in the milieu of post-transcriptional gene regulation by modulating the secondary and tertiary structure of RNA, thereby regulating RNA\RNA and RNA\protein interaction (39,40). Further, multiple lines of investigation from vertebrates show that D-E-A-D Box RNA helicases are essential for maintaining skeletal muscle mass, architecture, and function as well as muscle repair and regeneration via regulating ribosome biogenesis (41–43). Here, we report the function of DDX24, a D-E-A-D Box RNA helicase, in planarian head regeneration. *ddx24* was expressed in a subset of neoblasts, neoblasts primed for muscle fate, and also in the differentiated muscles. We custom generated a polyclonal antibody against DDX24 and found that the protein was particularly enriched in longitudinal and diagonal muscle fibers. Knockdown of *ddx24* resulted in muscle fiber disorganization and abnormal expression of anterior-pole markers like *zicA, foxD, and notum*, suggesting a defect in the anterior-pole specification**.** Loss of DDX24 also resulted in gross misregulation of many well-characterized patterning-control genes and positional-control genes, leading to defective regeneration. One such well-studied positional-control gene is *wnt1*. Although wound-induced expression of *wnt1* happens both in posterior and anterior blastema at early time-points of regeneration, this expression subsequently converges to the posterior tip by later stages of regeneration (44). However, in *ddx24* KD animals, Wnt activity is upregulated both in the posterior and anterior regenerating tissues compared to the controls. Modulating this Wnt activity by knocking down *β-catenin-1*, the effector molecule of this pathway, in the *ddx24* KD background, partially rescued the regeneration defect. Therefore, it is likely that DDX24 is

required for regulating Wnt activity essential for proper localization of signaling centers essential for regeneration.

Like many other tissues, muscle function was shown to be critically dependent on its translational landscape, which in turn is primarily controlled by regulating ribosome biogenesis (42,45–49). Knockdown of *ddx24* in planarians resulted in reduced levels of large subunit ribosomal RNA (28S rRNA) as well as reduced 80S ribosome peak. This aspect appears to be an evolutionarily conserved role of DDX24 (50,51). Since DDX24 protein was enriched in muscles, these results suggested that DDX24 could enable the functional state of these muscles by regulating their translational output via ribosome biogenesis.

RESULTS

DDX24 is necessary for anterior regeneration.

D-E-A-D box helicases are highly conserved RNA binding proteins that play critical roles in numerous aspects of RNA metabolism. We performed an RNAi screen aimed at finding different RNA helicases essential for regeneration in planarians. Here we report that SMED-DDX24, the planarian homolog of human DDX24, was one of D-E-A-D Box RNA helicases necessary for anterior regeneration (Figure1 figure supplement 1a). While planarians regenerate all missing tissues within 7 days post-amputation (DPA), *ddx24* knockdown (KD) animals failed to do so. All the control animals regenerated their eyespots by 7 DPA whereas *ddx24* KD animals lacked the eyespots (Figure 1a). Photoreceptor in *Schmidtea mediterranea* is characterized by the presence of pigment cup and photoreceptor neurons (PRN). Immunostaining with anti-arrestin antibody and RNA-FISH for *opsin*, which cumulatively marks the PRN, optic chaisma, and cell body of the PRN (52,53), showed defective

120 photoreceptor organization in the *ddx24* KD animals (Figure 1b). We then sought to investigate
121 the status of other organ systems in our knockdown animals. In planarians, the cephalic ganglia,
122 i.e., its brain, is a bilobed structure (54), which can be visualized by the staining with nuclear
123 dyes such as Hoechst or by immunostaining with anti- Gα q/11/14 antibody. In *ddx24* RNAi
124 animals, the planarian brain either failed to regenerate completely, or a rudimentary brain was
125 formed compared to the control animals (Figure 1c).
126 Planarian flatworms belong to the order tricladida characterized by the presence of three
127 primary gut branches- one anterior primary gut branch that splits pre-pharyngeally into two
128 posterior primary gut branches (55). dsRNA treated animals were amputated post-pharyngeally
129 such that the posterior gut branches merge and then subsequently regenerate the entire anterior
130 gut branch (Figure 1- figure supplement 1b). RNA in-situ for *mat*, a gut marker (56), clearly
131 showed that *ddx24* KD animals failed to regenerate the anterior branch of the intestine (Figure
132 1d). Also, no pharyngeal cavity (marked by Asterix *) was observed in these knockdown
133 animals. This was indicative of defective pharynx regeneration. Lack of pharynx in *ddx24* KD
134 animals was also corroborated by 6G10 staining that marks pharyngeal muscles (Figure 1-
135 figure supplement 1e) (57).
136 Together, our data shows that loss of DDX24 completely impaired anterior regeneration.
137 Posterior/tail regeneration was also defective in absence of DDX24 (Figure 1- figure
138 supplement 1f, g). Overall, DDX24 is necessary for regeneration in planarians.
139
140 **DDX24 protein is enriched in a subset of muscle fibers.**
141 Since we observed gross regeneration defects in *ddx24* knockdown, to better understand the
142 localization and function of DDX24, we custom generated a polyclonal antibody against the
143 peptide, SPKSLNADMQQKMRLKKLE, specific to planarian DDX24. Knockdown of *ddx24*
144 followed by western blot and immunostaining with this antibody showed decreased levels of

DDX24, thereby validating the efficacy and specificity of our antibody (Figure 2- figure supplement 2a-c). Immunostaining using this antibody prominently labeled body wall muscles (Figure 2a). Planarian body wall musculature (BWM) consists of three layers- circular, diagonal, and longitudinal muscle fibers (31). Our antibody stained the diagonal and longitudinal muscle fibers conspicuously. In contrast, circular muscle fibers showed a lower expression of DDX24 (Figure 2b). Overall, our immunofluorescence data showed that DDX24 was predominantly present in the longitudinal and diagonal muscle fibers compared to any other tissue in the animal. To further validate the enrichment of DDX24 in muscle, we employed double-RNA-FISH (dFISH) (58) to uncover the co-expression of *ddx24* with *collagen* and *bwm1*, bonafide pan-muscle markers in planarians (24,27,32). We found that a significant number of *ddx24+* cells were also positive for *collagen* (Figure 3a) and *bwm1* expression (Figure 3- figure supplement 3a). For instance, 65.8 ± 9.8% of *collagen+* cells and 63.4 ± 7.6% of *bwm1+* cells also expressed *ddx24*. This together with the immunofluorescence data demonstrated that DDX24 protein and its transcript are expressed in muscles. MyoD is the master transcription factor that specifies longitudinal muscle fibers in planarians (31). Since DDX24 protein was enriched in longitudinal muscles, we also validated this observation by performing double-RNA-FISH for *ddx24* and *myoD*. Co-localization experiments showed that 54.2 ± 0.7% of the *myoD+* cells also expressed *ddx24* (Figure 3b). NKX1.1 on the other hand specifies circular muscle fibers and DDX24 also had lower expression in these fibers compared to longitudinal or diagonal muscle fibers. In agreement with the latter observation, we found that a relatively lower percentage of *nkx1.1+* cells, i.e., 21.3 ± 7.8%, co-expressed *ddx24* (Figure 3- figure supplement 3b).

Previously published transcriptome data (59) revealed the expression of *ddx24* in planarian stem cells i.e., neoblasts. Immunostaining for DDX24 on FACS sorted X1 cells (proliferating neoblasts) showed the presence of DDX24 in a subset of these cells (Figure 2c). This

observation was further supported by the double-RNA-FISH, which showed that 22.1 ± 4.6% of *piwi-1*+ cells, a pan-neoblast marker, also expressed *ddx24* (Figure 3c). Since we found DDX24 protein in muscles and stem cells, we hypothesized that a fraction of the neoblasts that expressed the *ddx24* could be a neoblast population primed for muscle lineage. To test this, we performed double-RNA-FISH using *in situ* probes for *ddx24* and *collagen*, in combination with immunostaining using an antibody against PIWI-1 protein, a marker for pluripotent neoblasts and early progenitors (i.e., immediate neoblast progeny) (60). Our results showed that 36.5 ± 9.7% of *ddx24*-PIWI1 double-positive cells were also positive for *collagen* (Figure 3d). This suggested that a subset of *ddx24*+ neoblasts were indeed primed for muscle fate. This finding was further corroborated by multiple single-cell RNA sequencing datasets (61,62) which also show the expression of *ddx24* in the muscle primed neoblast population (Figure 3-figure supplementary 3e-g).

It is worth mentioning that even though single-cell RNA-seq datasets point towards the expression of *ddx24* transcript in other lineages, like the epidermis, gut, neural, and pharynx, our antibody did not detect DDX24 protein in any of these differentiated planarian tissues. However, in intact animals, DDX24 expression was detected in cells other than muscle fibers whose identity we were unable to determine (Figure 2- figure supplement 2d).

Loss of DDX24 leads to defective muscle fiber integrity and organization

Since DDX24 protein was enriched in muscles, we next investigated the status of muscle fibers in *ddx24* KD animals. Body wall muscle fibers run across the entire body wall column in planarians. Each fiber is continuous and these are of three kinds- circular, diagonal, and longitudinal (25,31). Loss of DDX24 led to a severe defect in muscle fiber organization and integrity (Figure 4 and Figure 4- figure supplement 4d). These indentations and fractures in muscle fiber architecture were predominately localized around the central region on both the

dorsal as well as on the ventral surface of the animal (Figure 4- figure supplement 4c video). Dark-field images and Hoechst staining revealed that there was no overall indentation or lesions on the surface of these animals (Figure 4 and Figure 1- figure supplement 1f) suggesting that this specific phenotype was restricted to the muscle compartment. Albeit at a lower frequency, we also observed these muscle fractures at the anterior tip of *ddx24* KD animals (Figure 4- figure supplement 4a). This was interesting because this region houses specialized muscle cells known as anterior pole cells which acts as the head-organizer essential for head regeneration (4,7–9). Further, we observed that the loss of DDX24 did not affect the expression of *collagen* suggesting that DDX24 was not necessary for *piwi1+* neoblasts to differentiate into *collagen+* muscles (Figure 4- figure supplement 4b). *myoD* levels too remained unchanged in absence of DDX24 (Figure 4- figure supplement 4j). On similar lines, even though DDX24 was also expressed by a population of neoblasts, we found that loss of DDX24 did not affect their maintenance, proliferation, or their fate commitment to different lineages (Figure 4- figure supplement 4e-i). Together, our data suggest that DDX24 predominantly functions at the level of muscle fiber organization rather than affecting gross muscle fate specification.

DDX24 is necessary for anterior pole re-specification during regeneration.

Head regeneration and patterning of different tissues within the head primordia is critically dependent on the spatial and temporal determination of the anterior pole. The anterior pole is marked by the combined expression of transcripts like *zicA*, *foxD*, *notum*, in a neoblast progeny committed for muscle lineage (7–9). This fate commitment occurs between 24 to 72 hours post-amputation (hpa) exclusively at anterior facing wounds. RNA-FISH for *ddx24* showed its expression in the anterior blastema by 72 hpa. Interestingly, we noted co-expression of *ddx24* with *zicA+ foxD+* anterior pole progenitors at this time point of regeneration (Figure 5- figure supplement 5a). We further noted co-expression of *ddx24* with *zicA+ foxD+* anterior pole in

intact animals (Figure 5a). Multiple single-cell RNA sequencing datasets further corroborated this observation that *ddx24* was indeed co-expressed by anterior pole cells- the expression of *ddx24* in the NB6 cluster (62) (Figure 3- figure supplement 3f) as well as co-expression of genes like *zicA, fst, prep, pbx, notum, sFPR-1, foxD, and nr4* in *ddx24+* single cells from Fincher et al., 2018 (61) (Figure 3- figure supplement 3g).

It is well established that loss of pole determinants like *zicA, foxD*, and *notum* leads to a failure in head regeneration (3,7–9). *ddx24* RNAi animals also failed to specify *zicA+ foxD+* pole cells by 72 hpa at the anterior tip (Figure 5b). Intriguingly, at the same timepoint, *ddx24* KD animals either failed to completely specify *notum+* anterior pole or showed gross mis-patterning of *notum* expression (Figure 5- figure supplement 5b). Next, we performed bulk RNA sequencing from *ddx24* KD and control animals to identify different genes and pathways mis-regulated after *ddx24* RNAi. We found that genes necessary for pole specification cum head regeneration like *pbx/extradenticle*, *follistatin* (*fst),* and *foxD* (5–7,9,63,64) were down-regulated *ddx24* knockdown animals (Figure 5- figure supplement 5d). We also compared our sequencing data with another recently published anterior pole enriched transcriptome dataset (65). This enabled us to identify two distinct cohorts of anterior pole enriched transcripts- one cohort was downregulated whereas the other was upregulated in absence of DDX24 (Figure 5-figure supplement 5e). These data, therefore, suggest that the genetic program associated with anterior pole specification during head regeneration is abnormal in *ddx24* knockdown animals. Defect in muscle fiber organization and pole specification suggested that positional-information re-specification was likely defective in absence of DDX24 (5–9,31). This is important because the expression of positional-control genes need re-wiring within the existing animal fragment during regeneration (23). This allows for re-specification of head-trunk-tail identities necessary for organogenesis, tissue-positioning, and tissue-patterning to proceed in a bonafide manner (13–15,66). Re-analyzing previously published single-cell RNA sequencing

data (61) suggested that a sizable population of *ddx24+* cells co-expressed many of these positional-control genes and patterning genes (Figure 3- figure supplement 3g). We then performed RNA-FISH for some of these genes like *ndl-3, ndl-5, sFRP-1, sFRP-2,* and *slit-1,* and found that their expression was mis-regulated in absence of DDX24 (Figure 5- figure supplement 5c). This finding was again corroborated by our bulk RNA-sequencing analysis that indeed many well-characterized positional-control genes and patterning genes such as *netrin-3, ndl-2, ndk, sFRP-1, slit-1, fz-4-2, fz-5/8-3,* and, *wnt-11-1* (16,22,23,67,68) were downregulated *ddx24* KD animals (Figure 5- figure supplement 5d). These observations thus indicate that DDX24 is required for the proper expression of positional control genes necessary for proper head regeneration and patterning in planarians.

DDX24 suppresses would-induced expression of *wnt1*.

Canonical WNT-βCATENIN signaling is required for tail specification with concomitant suppression of head identity throughout bilateria, including planarians (69–72). Failure of *ddx24* KD planarians to regenerate head hinted at the possibility of aberrant Wnt signaling in these animals. Although expression of *wnt1*, a canonical Wnt signaling ligand, at the wound site is a generic response to any wounding in planarians (44,73), head-regenerating wounds however completely suppress the expression of *wnt1* at the wound site by 24 to 30 hpa. Suppression of this *wnt1* expression at head-regenerating wounds is necessary for neoblasts to specify *zicA+ notum+* anterior-pole cells, in absence of which head regeneration fails (8,64). Upon RNA-FISH, we found that the number of wound-induced *wnt1+* cells was greatly increased in absence of DDX24 (Figure 5c and Figure 5- figure supplement 5f). In addition, our transcriptome data also revealed that the expression of *wnt-11-4/wntP3/wnt-4* (22,23), another canonical Wnt signaling ligand, was significantly upregulated in *ddx24* KD animals (fold-change (*ddx24* KD/Control KD) = 3.14; adjusted p-value = 0.0009). Therefore, it is likely

that the activity of canonical WNT-βCATENIN signaling is upregulated in absence of DDX24 and this could be one potential reason why *ddx24* KD planarians fail to regenerate their head. To further test this idea, we performed a double knockdown of *β-catenin-1* and *ddx24*. We decided to knockdown *β-catenin-1* because canonical Wnt ligands, WNT1 and WNT-11-4, both act via β-CATENIN-1 (22), a common effector of the canonical Wnt pathway. Approximately 54% of *β-catenin-1 ddx24* double knockdown animals regenerated at least one eyespot by the 10th day of regeneration whereas less than 5% of *ddx24* single knockdown animals did so (Figure 5d). Therefore, this partial rescue of *ddx24* RNAi phenotype by *β-catenin-1* RNAi supports the hypothesis that higher Wnt activity in *ddx24* KD animals is one potential reason why these animals fail to regenerate their head. This data is in alignment with previously published results that upregulation of Wnt activity (either through *fst* RNAi or *APC* RNAi) leads to defective head regeneration since a high Wnt environment leads to loss of *zicA+ notum+* anterior-pole cells (8,64), something we observe in *ddx24* KD animals as well.

ddx24 KD leads to downregulation of ribosomal RNA processing machinery

We next sought to uncover one potential sub-cellular mechanism how DDX24, an RNA helicase, could affect muscle architecture and function, thereby affecting whole-body regeneration. GO analysis of our bulk RNA sequencing data revealed that the expression of many genes associated with ribosomal RNA processing machinery was de-regulated in *ddx24* KD animals (Figure 6a). Mak5, the yeast homolog of DDX24, was shown to be essential for large subunit ribosomal RNA maturation (50,51,74). In planarians, the qRT-PCR analysis revealed ~40% downregulation in 28S rRNA levels upon *ddx24* KD whereas 18S rRNA levels remain nearly unchanged (Figure 6b). Therefore, our data hinted towards potential mis-regulation in translation mediated by reduced levels of mature 80S ribosomal. This was tested by performing polysome profiling on planarian lysates from control and knockdown animals.

As predicted, the 80S ribosome peak was reduced in the absence of DDX24, which is suggestive of defective ribosome assembly leading to a perturbed translational landscape (Figure 6c). Since DDX24 protein was enriched in body wall muscles, and a subset of X1 neoblasts, we speculated that defective ribosome biogenesis in *ddx24* KD animals was predominantly restricted to these specific compartments. Therefore, it is likely that muscle defects in *ddx24* KD animals, both in terms of muscle fiber organization as-well-as failure to specify anterior-pole cells, could be a result of defective translational machinery in these cells. In conclusion, our work highlights the role of translation regulation mediated by a D-E-A-D Box RNA helicase in whole-body regeneration via maintaining muscle form and function.

DISCUSSION

Planarians have a remarkable ability to undergo whole-body regeneration. Any part of their body lost to injury or amputation is functionally restored in a matter of weeks! It has therefore been a long-standing interest to understand the factors and mechanisms that enable this process. For example, successful polarity determination at the wound site is necessary for proper regeneration. The expression of a Wnt pathway antagonist *notum*, for instance, determines anterior polarity at an anterior-facing wound site (3). This process is followed by anterior pole re-specification. Anterior pole cells are marked by the co-expression of markers like- *notum, fst, foxD,* and *zicA* in neoblast progeny primed for muscle lineage (7–9). These clusters of cells are necessary for initiating head regeneration as well as positioning and patterning of different anterior tissues.

In planarians, muscles predominantly express all the pole determinants as well as other positional-control genes that are associated with head-trunk-tail identity re-specification within

the regenerating animal fragment (24). Muscles also serve as structural scaffolds for organ regeneration (26). In vertebrates, connective tissues, like fibroblasts, migrate to the wound site, generate different tissue types as well as display positional memory- processes essential for limb regeneration (75–82). Interestingly, in planarians, muscles have additional connective tissue type roles too. They express all the matrisome related genes- these ECM glycoproteins, *perlecan, hemicentin-1*, for example, are necessary for maintaining spatial positioning of different mesenchymal cell-types in these flatworms (27,28). However, the factors that underlie this tremendous functional versatility of planarian muscles remains poorly understood.

Previous studies in vertebrates have shown that regulating the translational landscape was necessary for maintaining the functional state, biomass, and architecture of muscles (42,45–49). Translation can be regulated by different post-transcriptional processes such as ribosome assembly, mRNA stability, and regulation of translation initiation and elongation (83–86). D-E-A-D box (DDX) helicases, a highly conserved family of RNA binding proteins and well-known regulators of different post-transcriptional and translational processes, were shown to be critical for myogenic fate and function (41–43,87,88). For example, in zebrafish, DDX27 is necessary for the proliferation and differentiation of myogenic progenitor cells to myofibers as well as for muscle repair and regeneration post-injury. DDX27 is essential for rRNA synthesis and ribosome assembly in these cells and *ddx27* knockout downregulates the translation of transcripts necessary for myogenesis (42).

We conducted an RNAi screen for different post-transcriptional gene regulators, including members from the D-E-A-D box RNA helicase family, in *Schmidtea mediterranea*, the go-to model system to study whole-body regeneration. Here, we report that SMED_DDX24, the *Schmidtea mediterranea* homolog of human DDX24, is essential for its regeneration. Although DDX24 is conserved across eukaryotes, little is known about the function of this protein in regulating various biological processes. In this study, we have mostly focused our effort to

345 understand how DDX24 governs head regeneration in planarians. We found that *ddx24* mRNA
346 is expressed by a population of neoblasts, neoblasts primed for muscle fate, and differentiated
347 muscles. However, the protein is highly enriched in body-wall muscle fiber, particularly
348 diagonal and longitudinal muscle fibers. We also detected the protein in a subset of neoblasts.
349 Although, the loss of DDX24 did not affect *piwi1*+ neoblasts, their maintenance, proliferation,
350 or their overt differentiation. However, the loss of DDX24 did severely affect muscle fiber
351 organization and integrity. This defect was observed both on the dorsal and the ventral surfaces
352 and with a lower frequency, on the tip of the regenerating head. Although *ddx24* was expressed
353 in a subset of stem cells primed for muscle fate, our transcriptome and RNA-FISH data
354 suggested that *ddx24* RNAi does not affect muscle lineage specification as such. Therefore, it
355 is likely that DDX24 is required for organizing muscle fibers and not for their overall fate
356 determination.
357 We also found the co-expression of *ddx24* with the anterior pole markers, both in intact and in
358 72-hour post-amputation head-regenerating animals. Besides, the loss of DDX24 eliminated
359 these pole cells too. This raised the possibility that DDX24 was required for anterior pole
360 determination. Moreover, *ddx24* KD animals had highly upregulated and ectopic expression of
361 wound-induced *wnt1*. This was interesting since a high level of Wnt activity is known to inhibit
362 the specification of *zicA*+ anterior pole cells, thereby leading to defective head regeneration
363 (8). Therefore, we modulated this ectopic Wnt signalling through *β-catenin-1* RNAi, the
364 effector molecule of this pathway. This led to the partial rescue of the eyeless phenotype
365 in *ddx24* RNAi animals. Hence, it is likely that the defective head regeneration in *ddx24* KD
366 animals is due to their inability to specify *zicA*+ anterior pole cells caused by higher levels of
367 wound-induced Wnt activity. A similar mechanism of action was also shown in *follistatin*
368 *(fst)* knockdown (66). Over induction of wound-induced *wnt1*+ cells in *fst* RNAi animals
369 impedes the formation of *notum*+ anterior pole, thereby leading to defective head-

regeneration. Besides, *wnt1* or *β-catenin-1* RNAi rectified *fst* RNAi phenotype as well. Interestingly, our data also showed reduced levels of *fst* and *notum* in *ddx24* KD. Although the specification of *foxD*+ anterior-pole cells is independent of WNT-βCATENIN signalling (7), elimination of *zicA* somehow eliminates *foxD* expression by 72-hour post-amputation (9). Therefore, this could be one possible explanation for why *ddx24* RNAi animals also failed to specify *foxD*+ pole cells. Furthermore, tail regeneration was also defective in absence of DDX24. Specification of *wnt1*+ posterior-pole is necessary for tail regeneration (44,68) and *ddx24* RNAi animals also had a very high level of ectopic *wnt1* expression at the tail-blastema. Although how this process unfolds is not understood, nevertheless it is very interesting that an abnormally high level of Wnt signalling could impede tail regeneration. Together, our data suggest that DDX24 plays an important role in modulating the levels of wound-induced Wnt activity, necessary for proper pole organization during regeneration.

The expression of many well-characterized positional-control genes was grossly mis-regulated in *ddx24* knockdown animals. Many of these genes are essential for tissue-positioning and tissue-patterning during regeneration, necessary for proper organogenesis. For example, *ndk* levels were downregulated in absence of DDX24. *ndk*, an FGF receptor-like gene (86), regulates cephalic ganglia regeneration by delineating its posterior boundary. Another example would be that of *slit-1*, an evolutionarily conserved gene necessary for proper medial-lateral positioning of regenerating organs (67), whose levels were also reduced in *ddx24* knockdown. It is worth recapitulating here that- (i) all these positional-control genes are predominantly expressed by muscles and (ii) loss of muscle fibers (for example *myoD* RNAi (31)) or loss of anterior pole determinants (7–9) results in abnormal positional-control gene expression. Therefore, to summarize, our study shows a novel role of DDX24 in regulating muscle fiber organization, anterior pole determination, and positional-information re-specification thereby enabling head regeneration in planarians.

Mak5, the yeast homolog of DDX24 is necessary for large subunit ribosome RNA biogenesis, in effect ribosome biogenesis (50,51,74). In planarians, we investigated the potential role of DDX24 on 28S rRNA levels. Although 18S rRNA levels remained unperturbed, the knockdown of *ddx24* led to a decrease in levels of 28S rRNA which subsequently led to a reduction in the 80S monosome peak. DDX24 knockdown, therefore, alters the translational landscape in planarians. In vertebrates, it has been shown that regulating the translatome is important for maintaining the fate and function of skeletal muscles. On similar lines, our study highlights the possibility that DDX24 regulates ribosomal biogenesis in planarian muscle cells via regulating 28S rRNA levels. This regulation in turn could be important for muscle function. However, the mechanism by which DDX24 regulates ribosome biogenesis remains to be investigated. D-E-A-D box RNA helicases are versatile proteins- they can directly interact with proteins as well as different species of RNA to elicit their specific function in a context-dependent fashion. Future interactome studies of DDX24 would help to understand precise molecular underpinnings through which it regulates whole-body regeneration in planarians.

MATERIAL & METHODS

Animal husbandry

The sexual strain of *Schmidtea mediterranea* was used in this study. All animals were kept in 1X planaria media (1.6 mM NaCl, 1.0 mM CaCl2, 1.0 mM MgSO4, 0.1 mM MgCl2, 0.1 mM KCl, and 1.2 mM NaHCO3 pH adjusted to 7.0) in 20 degrees. Planarians were starved for at least one week before any experiment.

RNA Interference

Sequence of *ddx24* (transcript id: dd_v6_Smed_7310_0_1) can be found on PlanMine (http://planmine.mpi-cbg.de) (59). Primer pair used to amplify *ddx24*: forward primer- 5'-TGCCAACAGCAAGAACTCAG-3'; reverse primer- 5'GACGGTGCGTTTTTCTTCTC-3'.

dsRNA synthesis and feeding were performed as described by Rouhana & colleagues (89). dsRNA against the green fluorescent protein (GFP) was used as RNAi control. Animals were fed three dsRNA thrice with a gap of three days after each feed. On the fourth day post last feed planarians were amputated post pharyngeal to generate tail fragments. 1.5µg of dsRNA per 10 µL beef-extract was used to make the food-dsRNA mix. qPCR primer pair used to check *ddx24* knockdown: forward primer- 5'- GGATTTTTGAAACCGACACA-3'; reverse primer 5'-CCCAAATGCTAATGTTTTGC- 3'. Our transcriptome data shows that *ddx24* KD leads to the downregulation of *ddx24's* expression alone without affecting the transcript levels of other DEAD box RNA helicases which also shows the specificity of the dsRNA used for the study (Figure1 figure supplement 1 c,d)

RNA insitu hybridisation and immunostaining

RNA- insitu hybridisation was performed as described by King and Newmark (58). RNA-FISH for *ddx24* was always performed using a cocktail of two non-overlapping fluorescein-labeled riboprobes. The primer pair used to generate the first set of riboprobe is- forward: 5'-TTGCGTGGAATGACGATGAG-3'; reverse: 5'-AATGTGGCCGAAAACACGAG-3', and primer pair used to generate the second set of riboprobe is- forward: 5'-TGGCAGCAAGAGGTTTGGAT-3'; reverse: 5'-GTGGCCAGAAAGAGGGGACT-3'. The final concentration of riboprobes used was 1ng/ µL. The specificity of the riboprobes against

442 *ddx24* mRNA was validated by performing RNA FISH one week after *ddx24* RNAi (Figure 3
443 figure supplement 3 c, d)
444 Immunostaining for Arrestin (a kind gift from Prof. Kiyokazu Agata), 6G10, SMED-PIWI1,
445 and H3P was performed as described by previous papers from our lab (90–92). Anti- Gα
446 q/11/14 (G-7) (1:200 Santa Cruz Biotechnology, sc-365906) antibody staining was performed
447 in formaldehyde-fixed samples after RNA-FISH was performed on them. Fluorophore
448 conjugated anti-mouse secondary antibody (Life Technologies) was used at a dilution of
449 1:1000, for two hours at room temperature.

450 For anti-DDX24 antibody immunofluorescence, planarians were sacrificed in 5% N-Acetyl
451 Cysteine in 1X PBS for 7 minutes, rinsed 2X with 1X PBS, and fixed in ice-cold meth-Carnoy
452 solution (methanol: chloroform: acetic acid in 6:3:1 ratio by volume) for 45 minutes in cold-
453 room with mild nutation post which they were washed multiple times with cold methanol and
454 eventually brought to room temperature. Animals were gradually rehydrated in
455 graded methanol-0.5% PBSTx. 6% H2O2 (either in 1X PBS or 100% methanol. Muscle
456 staining is better with methanol bleach whereas detection of the "other" cell types happens
457 better with PBS bleach) under bright light was used to bleach animals. Rabbit anti-DDX24
458 antibody was used at 1:50 dilution and incubated at 4 degrees for 24 hours. Anti-Rabbit-HRP
459 (1:1000, Cell Signaling Technology 7074) was used as the secondary antibody. Development
460 was performed using tyramide signal amplification. Hoechst 33342 (1:1000, Invitrogen) was
461 used to stain nuclei. Samples were mounted using Scale A2 as described by Adler and
462 colleagues (93) and stored at 4 degrees.

463
464
465
466

Antibody Generation and Western Blotting

Rabbit anti-DDX24 antibody was generated against the peptide CSPKSLNADMQQKMRLKKLE specific to SMED-DDX24 and affinity-purified (Abgenex, Bhubaneswar India). Western blotting was performed as described by Owlarn and colleagues (94). DDX24 antibody was used at 1:1000 dilution. Rabbit Beta-Actin antibody (Cell Signaling Technology 4967S) and Rabbit SMED-PIWI1 antibody (60) were used at 1:2000 & 1:1000 dilution respectively.

Image Acquisition

All brightfield images were taken Olympus SZX16. Confocal images were acquired on an Olympus FV 3000 laser scanning microscope. Images were processed using Fiji. (https://imagej.net/Fiji). All cell counting was performed manually.

RNA extraction, cDNA synthesis, and qRT-PCR analysis

For any experiment, ~10 animals were used to extract RNA using TRIzol™ reagent (Invitrogen). cDNA was synthesised using SuperScript™ III Reverse Transcriptase (Invitrogen) using random hexamer primers. Maxima SYBR Green/ROX qPCR Master Mix (2X) (ThermoFisher Scientific) was used for qRT-PCR experiments.

qPCR primer pairs (5’ to 3’) used are:

18S rRNA-GGCGGTATTTTGATGACTCTGG (F), GTGGATGTGGTAGCCGTTTCTC (R)

28S rRNA-GATGCTTCCTATGAGTCGGATTG (F), CGGCTTCACTCGTTTACCTCTAA (R)

ddx24- GGATTTTTGAAACCGACACA (F), CCCAAATGCTAATGTTTTGC (R)

Actin- GCTCCACTCAATCCAAAAGC (F), TCAAATCTCTACCGGCCAAG (R)

Each experiment was repeated three times independently. Actin was used for normalisation. Unpaired t-test was used for inferencing statistical significance. All graph was plotted on GraphPad Prism 6.

Polysome profiling

3 DPA planarian tails were soaked in cycloheximide (CHX) for 2 hours at 100 µg/ml final concentration in 1X planaria media. After this, they were macerated in cold CMF (calcium-magnesium free media) to dissociate them into cells. The cells were then pelleted by spinning at 300g for 10 minutes in a swinging bucket. The supernatant was discarded and cells were resuspended in 400 µl of polysome lysis buffer (200mM KCL, 5mM $MgCl_2$, 0.01% TritonX-100, 20mM Tris-Cl pH 7.5, 1X Protease Inhibitor Cocktail, 40U/mL RNAse inhibitor, and 100 µg/ml CHX). Cells were incubated in lysis buffer for 30 min on ice, vigorously pipetted and vortexed. This was then centrifuged at 13,000g for 30 minutes. The supernatant was collected and was loaded onto a sucrose gradient (15% to 45%) and centrifuged at 40,000 RPM for 2 to 2.5 hours at 4°C. The sucrose gradient was then loaded onto an ISCO Teledyne UA-6 Absorbance Detector. Sixty percent sucrose was pumped from below to push the sucrose gradient to the UV chamber. The sensitivity parameter of the machine was set at 0.5.

Transcriptome analysis

RNA was extracted from 3 DPA tail fragments and transcriptome library was prepared using NEBNext® Ultra™ II Directional RNA Library Prep with Sample Purification Beads (catalogue no-E7765L) kit and sequenced in Illumina HiSeq 2500 machine. All the samples were sequenced (as single-end) in biological replicates. Approximately 28 to 31 million reads were sequenced for every sample. These reads were adapter trimmed using Trimmomatic (95)

514 and mapped to rRNA and other contamination databases. Reads that did not align with these
515 databases were taken for further analysis. We used reference-based transcriptome assembly
516 algorithms Hisat2 v2.1.0 (96); Cufflinks v2.2.1 (97) and Cuffdiff v2.2.1 (98) to identify
517 differentially expressed transcripts. We used Hisat2 (-q -p 8 --min-intronlen 50 --max-intronlen
518 250000 --dta-cufflinks --new-summary --summary-file) to align the reads back to dd_Smes_G4
519 (99) assembly of *Schmidtea mediterranea* genome. Around 81-84% of reads were mapped to
520 dd_Smes_G4 genome. We used samtools to obtain sorted bam files. The mapped reads were
521 assembled using Cufflinks (-p -o -b -u -N --total-hits-norm -G) with the most recent and well-
522 annotated SMEST transcriptome as reference. We used cuffmerge to merge the gene list across
523 different conditions. We identified differentially expressed genes using Cuffdiff module (-p -o
524 ./ -b -u -N --total-hits-norm -L) and considered genes with adjusted p-value <0.05 as
525 significance cut-off. Genes with significant p-value and at least two-fold up/down regulation
526 were considered for further analysis. We did pathway analysis & gene-ontology analysis for
527 these selected up/down regulated transcripts using GSEA (100,101). We used a customized
528 perl script for all the analyses used in this study. We used R ggplot2 (102), pHeatmap and
529 CummeRbund (103) library for plotting. Different planarian cell-type markers were obtained
530 from the available single-cell transcriptome data (61).

531

532 **Single-cell transcriptome analysis**

533 We used single-cell transcriptome published from Peter Reddien's lab (61) to extract the cells
534 that express *ddx24*. We used the data matrix submitted in SRA to extract only the cells that
535 express *ddx24*. We found 3929 cells (out of 50,563 cells) expressing *ddx24* transcript in the
536 single-cell transcriptome. We re-analyzed the single-cell data as described in Ross and
537 colleagues (104). We used Seurat (https://satijalab.org/seurat/), an R package to analyze the
538 single-cell transcriptome for the cells that express *ddx24* mRNA (105,106). Based on the

markers from Fincher *et al.*, 2018, we classified the UMAP clusters as cell types. We used LogNormalize method of Seurat to normalize the dataset which was further scaled (linear transformation) using Seurat. This scaled value was further log-transformed and plotted as a heatmap for genes of interest. We used R ggplot2 GMD and heatmap.2 to derive all the plots.

Fluorescence-activated cell sorting (FACS)

FACS was performed as described by Wagner and colleagues (56).

ACKNOWLEDGMENT

We are grateful to Prof. Apurva Sarin for her critical comments and for proofreading our manuscript. SRS and VKD thank NCBS-inStem Ph.D. fellowship for funding. MMH is supported by DBT-JRF and VL is supported by CSIR-SRF. AJ and SS thank inStem for funding. We thank all the members of the Palakodeti and Sowdhamini labs for their constant support, critique, encouragement, and feedback, especially Dhiru Bansal, Giulia Moreni, Sayan Biswas, and Snehal Karpe for helping with experiments. We are grateful to Nishan Shettigar and Anirudh Chakravarthy from Akash Gulyani's lab for sharing their unpublished anti- Gα q/11/14 antibody staining protocol (Shettigar et al., 2020, under review) and to Prof. Kiyokazu Agata for generously gifting us anti-arrestin antibody. Authors acknowledge the in-house central imaging and flow cytometry facility (CIFF) and NGS facility (especially Awadhesh Pandit) for constant technical support. The work was funded by NCBS core grants and JC Bose fellowship to RS (SB/S2/JC-071/2015) and DST Swarnajayanti fellowship (DST/SJF/LSA-02/2015-16) and inStem core grants awarded to DP.

COMPETING INTERESTS

None declared

AUTHOR CONTRIBUTIONS

Conceptualization: Souradeep R. Sarkar, Dasaradhi Palakodeti.

Data curation: Souradeep R. Sarkar, Vairavan Laxmanan.

Formal analysis: Souradeep R. Sarkar, Vairavan Laxmanan.

Funding acquisition: Ramanathan Sowdhamini, Dasaradhi Palakodeti.

Investigation: Souradeep R. Sarkar, Vinay Kumar Dubey, Anusha Jahagirdar, Mohamed Mohamed Haroon, Sai Sowndarya.

Methodology: Souradeep R. Sarkar

Project administration: Souradeep R. Sarkar.

Resources: Ramanathan Sowdhamini, Dasaradhi Palakodeti.

Software: Vairavan Laxmanan.

Supervision: Ramanathan Sowdhamini, Dasaradhi Palakodeti.

Validation: Souradeep R. Sarkar, Anusha Jahagirdar, Mohamed Mohamed Haroon.

Visualization: Souradeep R. Sarkar.

Writing – original draft: Souradeep R. Sarkar.

Writing – review & editing: Souradeep R. Sarkar, Vairavan Laxmanan, Vinay Kumar Dubey, Anusha Jahagirdar, Mohamed Mohamed Haroon, Dasaradhi Palakodeti.

583 **REFERENCES**

584 1. Reddien PW, Sánchez Alvarado A. Fundamentals of planarian regeneration. Annual
585 Review of Cell and Developmental Biology. 2004.

586 2. Rink JC. Stem cells, patterning and regeneration in planarians: Self-organization at the
587 organismal scale. In: Methods in Molecular Biology. 2018.

588 3. Petersen CP, Reddien PW. Polarized notum activation at wounds inhibits Wnt function
589 to promote planarian head regeneration. Science (80-). 2011;

590 4. Felix DA, Aboobaker AA. The TALE class homeobox gene Smed-prep defines the
591 anterior compartment for head regeneration. PLoS Genet. 2010;

592 5. Chen CCG, Wang IE, Reddien PW. pbx is required for pole and eye regeneration in
593 planarians. Dev. 2013;

594 6. Blassberg RA, Felix DA, Tejada-Romero B, Aziz Aboobaker A. PBX/extradenticle is
595 required to re-establish axial structures and polarity during planarian regeneration.
596 Dev. 2013;

597 7. Scimone ML, Lapan SW, Reddien PW. A forkhead Transcription Factor Is Wound-
598 Induced at the Planarian Midline and Required for Anterior Pole Regeneration. PLoS
599 Genet. 2014;

600 8. Vásquez-Doorman C, Petersen CP. zic-1 Expression in Planarian Neoblasts after
601 Injury Controls Anterior Pole Regeneration. PLoS Genet. 2014;

602 9. Vogg MC, Owlarn S, Pérez Rico YA, Xie J, Suzuki Y, Gentile L, et al. Stem cell-
603 dependent formation of a functional anterior regeneration pole in planarians requires
604 Zic and Forkhead transcription factors. Dev Biol. 2014;

10. Oderberg IM, Li DJ, Scimone ML, Gaviño MA, Reddien PW. Landmarks in Existing Tissue at Wounds Are Utilized to Generate Pattern in Regenerating Tissue. Curr Biol. 2017;

11. Sureda-Gomez M, Adell T. Planarian organizers. Seminars in Cell and Developmental Biology. 2019.

12. Sander K, Faessler PE. Introducing the Spemann-Mangold organizer: Experiments and insights that generated a key concept in developmental biology. International Journal of Developmental Biology. 2001.

13. Hill EM, Petersen CP. Wnt/Notum spatial feedback inhibition controls neoblast differentiation to regulate reversible growth of the planarian brain. Dev. 2015;

14. Hill EM, Petersen CP. Positional information specifies the site of organ regeneration and not tissue maintenance in planarians. Elife. 2018;

15. Lander R, Petersen CP. Wnt, Ptk7, and FGFRL expression gradients control trunk positional identity in planarian regeneration. Elife. 2016;

16. Scimone ML, Cote LE, Rogers T, Reddien PW. Two FGFRL-Wnt circuits organize the planarian anteroposterior axis. Elife. 2016;

17. Wurtzel O, Oderberg IM, Reddien PW. Planarian Epidermal Stem Cells Respond to Positional Cues to Promote Cell-Type Diversity. Dev Cell. 2017;

18. Atabay KD, LoCascio SA, de Hoog T, Reddien PW. Self-organization and progenitor targeting generate stable patterns in planarian regeneration. Science (80-). 2018;

19. Reddien PW. The Cellular and Molecular Basis for Planarian Regeneration. Cell. 2018.

627 20. Adell T, Cebrià F, Saló E. Gradients in planarian regeneration and homeostasis. Cold
628 Spring Harbor perspectives in biology. 2010.

629 21. Sureda-Gómez M, Martín-Durán JM, Adell T. Localization of planarian β-CATENIN-
630 1 reveals multiple roles during anterior-posterior regeneration and organogenesis. Dev.
631 2016;

632 22. Stückemann T, Cleland JP, Werner S, Thi-Kim Vu H, Bayersdorf R, Liu SY, et al.
633 Antagonistic Self-Organizing Patterning Systems Control Maintenance and
634 Regeneration of the Anteroposterior Axis in Planarians. Dev Cell. 2017;

635 23. Gurley KA, Elliott SA, Simakov O, Schmidt HA, Holstein TW, Alvarado AS.
636 Expression of secreted Wnt pathway components reveals unexpected complexity of the
637 planarian amputation response. Dev Biol. 2010;

638 24. Witchley JN, Mayer M, Wagner DE, Owen JH, Reddien PW. Muscle cells provide
639 instructions for planarian regeneration. Cell Rep. 2013;

640 25. Cebrià F. Planarian body-wall muscle: Regeneration and function beyond a simple
641 skeletal support. Frontiers in Cell and Developmental Biology. 2016.

642 26. Adler CE, Sánchez Alvarado A. PHRED-1 is a divergent neurexin-1 homolog that
643 organizes muscle fibers and patterns organs during regeneration. Dev Biol. 2017;

644 27. Cote LE, Simental E, Reddien PW. Muscle functions as a connective tissue and source
645 of extracellular matrix in planarians. Nat Commun. 2019;

646 28. Lindsay-Mosher N, Chan A, Pearson BJ. Planarian EGF repeat-containing genes
647 megf6 and hemicentin are required to restrict the stem cell compartment. PLoS Genet.
648 2020;

649 29. Reddien PW, Bermange AL, Murfitt KJ, Jennings JR, Sánchez Alvarado A.

650 Identification of genes needed for regeneration, stem cell function, and tissue
651 homeostasis by systematic gene perturbation in planaria. Dev Cell. 2005;

652 30. Cowles MW, Brown DDR, Nisperos S V., Stanley BN, Pearson BJ, Zayas RM.
653 Genome-wide analysis of the bHLH gene family in planarians identifies factors
654 required for adult neurogenesis and neuronal regeneration. Dev. 2013;

655 31. Lucila Scimone M, Cote LE, Reddien PW. Orthogonal muscle fibres have different
656 instructive roles in planarian regeneration. Nature. 2017;

657 32. Scimone ML, Wurtzel O, Malecek K, Fincher CT, Oderberg IM, Kravarik KM, et al.
658 foxF-1 Controls Specification of Non-body Wall Muscle and Phagocytic Cells in
659 Planarians. Curr Biol. 2018;

660 33. Halbeisen RE, Galgano A, Scherrer T, Gerber AP. Post-transcriptional gene
661 regulation: From genome-wide studies to principles. Cellular and Molecular Life
662 Sciences. 2008.

663 34. Rouhana L, Shibata N, Nishimura O, Agata K. Different requirements for conserved
664 post-transcriptional regulators in planarian regeneration and stem cell maintenance.
665 Dev Biol. 2010;

666 35. Carpenter S, Ricci EP, Mercier BC, Moore MJ, Fitzgerald KA. Post-transcriptional
667 regulation of gene expression in innate immunity. Nature Reviews Immunology. 2014.

668 36. Weil TT. Post-transcriptional regulation of early embryogenesis. F1000Prime Rep.
669 2015;

670 37. Corbett AH. Post-transcriptional regulation of gene expression and human disease.
671 Current Opinion in Cell Biology. 2018.

672 38. Krishna S, Palakodeti D, Solana J. Post-transcriptional regulation in planarian stem

673 cells. Seminars in Cell and Developmental Biology. 2019.

674 39. Rocak S, Linder P. Dead-box proteins: The driving forces behind RNA metabolism.
675 Nature Reviews Molecular Cell Biology. 2004.

676 40. Jankowsky E. RNA helicases at work: Binding and rearranging. Trends in
677 Biochemical Sciences. 2011.

678 41. Jones K, Wei C, Schoser B, Meola G, Timchenko N, Timchenko L. Reduction of toxic
679 RNAs in myotonic dystrophies type 1 and type 2 by the RNA helicase p68/DDX5.
680 Proc Natl Acad Sci U S A. 2015;

681 42. Bennett AH, O'Donohue MF, Gundry SR, Chan AT, Widrick J, Draper I, et al. RNA
682 helicase, DDX27 regulates skeletal muscle growth and regeneration by modulation of
683 translational processes. PLoS Genet. 2018;

684 43. Zhang L, Yang Y, Li B, Scott IC, Lou X. The DEAD-box RNA helicase Ddx39ab is
685 essential for myocyte and lens development in zebrafish. Development. 2018;

686 44. Petersen CP, Reddien PW. A wound-induced Wnt expression program controls
687 planarian regeneration polarity. Proc Natl Acad Sci U S A. 2009;

688 45. Jolicoeur C, Noël J, Brakier-Gingras L. The 60S ribosomal subunit is altered in the
689 skeletal muscle of dystrophic hamsters. Biochem Biophys Res Commun. 1983;

690 46. Ohanna M, Sobering AK, Lapointe T, Lorenzo L, Praud C, Petroulakis E, et al.
691 Atrophy of S6K1-/- skeletal muscle cells reveals distinct mTOR effectors for cell cycle
692 and size control. Nat Cell Biol. 2005;

693 47. Machida M, Takeda K, Yokono H, Ikemune S, Taniguchi Y, Kiyosawa H, et al.
694 Reduction of ribosome biogenesis with activation of the mTOR pathway in denervated
695 atrophic muscle. J Cell Physiol. 2012;

48. Chaillou T, Kirby TJ, Mccarthy JJ. Ribosome Biogenesis: Emerging Evidence for a Central Role in the Regulation of Skeletal Muscle Mass. J Cell Physiol. 2014;

49. Marabita M, Baraldo M, Solagna F, Ceelen JJM, Sartori R, Nolte H, et al. S6K1 Is Required for Increasing Skeletal Muscle Force during Hypertrophy. Cell Rep. 2016;

50. Zagulski M, Kressler D, Bécam AM, Rytka J, Herbert CJ. Mak5p, which is required for the maintenance of the M1 dsRNA virus, is encoded by the yeast ORF YBR142w and is involved in the biogenesis of the 60S subunit of the ribosome. Mol Genet Genomics. 2003;

51. Brüning L, Hackert P, Martin R, Davila Gallesio J, Aquino GRR, Urlaub H, et al. RNA helicases mediate structural transitions and compositional changes in pre-ribosomal complexes. Nat Commun. 2018;

52. Agata K, Soejima Y, Kato K, Kobayashi C, Umesono Y, Watanabe K. Structure of the planarian central nervous system (CNS) revealed by neuronal cell markers. Zoolog Sci. 1998;

53. Shettigar N, Joshi A, Dalmeida R, Gopalkrishna R, Chakravarthy A, Patnaik S, et al. Hierarchies in light sensing and dynamic interactions between ocular and extraocular sensory networks in a flatworm. Sci Adv. 2017;

54. Ross KG, Currie KW, Pearson BJ, Zayas RM. Nervous system development and regeneration in freshwater planarians. Wiley Interdisciplinary Reviews: Developmental Biology. 2017.

55. Forsthoefel DJ, Park AE, Newmark PA. Stem cell-based growth, regeneration, and remodeling of the planarian intestine. Dev Biol. 2011;

56. Wagner DE, Wang IE, Reddien PW. Clonogenic neoblasts are pluripotent adult stem

719 cells that underlie planarian regeneration. Science (80-). 2011;

720 57. Ross KG, Omuro KC, Taylor MR, Munday RK, Hubert A, King RS, et al. Novel
721 monoclonal antibodies to study tissue regeneration in planarians. BMC Dev Biol.
722 2015;

723 58. King RS, Newmark PA. In situ hybridization protocol for enhanced detection of gene
724 expression in the planarian Schmidtea mediterranea. BMC Dev Biol. 2013;

725 59. Brandl H, Moon HK, Vila-Farré M, Liu SY, Henry I, Rink JC. PlanMine - A mineable
726 resource of planarian biology and biodiversity. Nucleic Acids Res. 2016;

727 60. Guo T, Peters AHFM, Newmark PA. A bruno-like Gene Is Required for Stem Cell
728 Maintenance in Planarians. Dev Cell. 2006;

729 61. Fincher CT, Wurtzel O, de Hoog T, Kravarik KM, Reddien PW. Cell type
730 transcriptome atlas for the planarian Schmidtea mediterranea. Science (80-). 2018;

731 62. Zeng A, Li H, Guo L, Gao X, McKinney S, Wang Y, et al. Prospectively Isolated
732 Tetraspanin + Neoblasts Are Adult Pluripotent Stem Cells Underlying Planaria
733 Regeneration. Cell. 2018;

734 63. Roberts-Galbraith RH, Newmark PA. Follistatin antagonizes Activin signaling and
735 acts with Notum to direct planarian head regeneration. Proc Natl Acad Sci U S A.
736 2013;

737 64. Tewari AG, Stern SR, Oderberg IM, Reddien PW. Cellular and Molecular Responses
738 Unique to Major Injury Are Dispensable for Planarian Regeneration. Cell Rep. 2018;

739 65. Li DJ, McMann CL, Reddien PW. Nuclear receptor NR4A is required for patterning at
740 the ends of the planarian anterior-posterior axis. Elife. 2019;

741 66. Gaviño MA, Wenemoser D, Wang IE, Reddien PW. Tissue absence initiates
742 regeneration through Follistatin-mediated inhibition of Activin signaling. Elife. 2013;

743 67. Cebrià F, Guo T, Jopek J, Newmark PA. Regeneration and maintenance of the
744 planarian midline is regulated by a slit orthologue. Dev Biol. 2007;

745 68. Sureda-Gómez M, Pascual-Carreras E, Adell T. Posterior wnts have distinct roles in
746 specification and patterning of the planarian posterior region. Int J Mol Sci. 2015;

747 69. Petersen CP, Reddien PW. Wnt Signaling and the Polarity of the Primary Body Axis.
748 Cell. 2009.

749 70. Petersen CP, Reddien PW. Smed-βcatenin-1 is required for anteroposterior blastema
750 polarity in planarian regeneration. Science (80-). 2008;

751 71. Adell T, Salò E, Boutos M, Bartscherer K. Smed-Evi/Wntless is required for β-
752 catenin-dependent and -independent processes during planarian regeneration.
753 Development. 2009;

754 72. Gurley KA, Rink JC, Alvarado AS. β-catenin defines head versus tail identity during
755 planarian regeneration and homeostasis. Science (80-). 2008;

756 73. Wenemoser D, Lapan SW, Wilkinson AW, Bell GW, Reddien PW. A molecular
757 wound response program associated with regeneration initiation in planarians. Genes
758 Dev. 2012;

759 74. Granneman S, Bernstein KA, Bleichert F, Baserga SJ. Comprehensive Mutational
760 Analysis of Yeast DEXD/H Box RNA Helicases Required for Small Ribosomal
761 Subunit Synthesis. Mol Cell Biol. 2006;

762 75. Kalluri R, Zeisberg M. Fibroblasts in cancer. Nature Reviews Cancer. 2006.

763 76. Rinn JL, Bondre C, Gladstone HB, Brown PO, Chang HY. Anatomic demarcation by
764 positional variation in fibroblast gene expression programs. PLoS Genet. 2006;

765 77. Kragl M, Knapp D, Nacu E, Khattak S, Maden M, Epperlein HH, et al. Cells keep a
766 memory of their tissue origin during axolotl limb regeneration. Nature. 2009.

767 78. Murphy MM, Lawson JA, Mathew SJ, Hutcheson DA, Kardon G. Satellite cells,
768 connective tissue fibroblasts and their interactions are crucial for muscle regeneration.
769 Development. 2011;

770 79. Nacu E, Glausch M, Le HQ, Damanik FFR, Schuez M, Knapp D, et al. Connective
771 tissue cells, but not muscle cells, are involved in establishing the proximo-distal
772 outcome of limb regeneration in the axolotl. Dev. 2013;

773 80. Wu Y, Wang K, Karapetyan A, Fernando WA, Simkin J, Han M, et al. Connective
774 Tissue Fibroblast Properties Are Position-Dependent during Mouse Digit Tip
775 Regeneration. PLoS One. 2013;

776 81. McCusker CD, Diaz-Castillo C, Sosnik J, Q. Phan A, Gardiner DM. Cartilage and
777 bone cells do not participate in skeletal regeneration in Ambystoma mexicanum limbs.
778 Dev Biol. 2016;

779 82. Gerber T, Murawala P, Knapp D, Masselink W, Schuez M, Hermann S, et al. Single-
780 cell analysis uncovers convergence of cell identities during axolotl limb regeneration.
781 Science (80-). 2018;

782 83. Chenette DM, Cadwallader AB, Antwine TL, Larkin LC, Wang J, Olwin BB, et al.
783 Targeted mRNA Decay by RNA Binding Protein AUF1 Regulates Adult Muscle Stem
784 Cell Fate, Promoting Skeletal Muscle Integrity. Cell Rep. 2016;

785 84. Zismanov V, Chichkov V, Colangelo V, Jamet S, Wang S, Syme A, et al.

786 Phosphorylation of eIF2α is a Translational Control Mechanism Regulating Muscle
787 Stem Cell Quiescence and Self-Renewal. Cell Stem Cell. 2016;

788 85. Abbadi D, Yang M, Chenette DM, Andrews JJ, Schneider RJ. Muscle development
789 and regeneration controlled by AUF1-mediated stage-specific degradation of fate-
790 determining checkpoint mRNAs. Proc Natl Acad Sci U S A. 2019;

791 86. Lin Y, Li F, Huang L, Polte C, Duan H, Fang J, et al. eIF3 Associates with 80S
792 Ribosomes to Promote Translation Elongation, Mitochondrial Homeostasis, and
793 Muscle Health. J Clean Prod. 2020;

794 87. Caretti G, Schiltz RL, Dilworth FJ, Di Padova M, Zhao P, Ogryzko V, et al. The RNA
795 Helicases p68/p72 and the Noncoding RNA SRA Are Coregulators of MyoD and
796 Skeletal Muscle Differentiation. Dev Cell. 2006;

797 88. Cauchi RJ, Davies KE, Liu JL. A motor function for the DEAD-box RNA helicase,
798 Gemin3, in Drosophila. PLoS Genet. 2008;

799 89. Rouhana L, Weiss JA, Forsthoefel DJ, Lee H, King RS, Inoue T, et al. RNA
800 interference by feeding in vitro-synthesized double-stranded RNA to planarians:
801 Methodology and dynamics. Dev Dyn. 2013;

802 90. Sasidharan V, Marepally S, Elliott SA, Baid S, Lakshmanan V, Nayyar N, et al. The
803 miR-124 family of microRNAs is crucial for regeneration of the brain and visual
804 system in the planarian schmidtea mediterranea. Dev. 2017;

805 91. Bansal D, Kulkarni J, Nadahalli K, Lakshmanan V, Krishna S, Sasidharan V, et al.
806 Cytoplasmic poly (A)-binding protein critically regulates epidermal maintenance and
807 turnover in the planarian schmidtea mediterranea. Dev. 2017;

808 92. Sarkar A, Mukundan N, Sowndarya S, Dubey VK, Babu R, Lakshmanan V, et al.

809 Serotonin is essential for eye regeneration in planaria Schmidtea mediterranea. FEBS
810 Lett. 2019;

811 93. Adler CE, Seidel CW, McKinney SA, Sánchez Alvarado A. Selective amputation of
812 the pharynx identifies a FoxA-dependent regeneration program in planaria. Elife.
813 2014;

814 94. Owlarn S, Klenner F, Schmidt D, Rabert F, Tomasso A, Reuter H, et al. Generic
815 wound signals initiate regeneration in missing-tissue contexts. Nat Commun. 2017;

816 95. Bolger AM, Lohse M, Usadel B. Trimmomatic: A flexible trimmer for Illumina
817 sequence data. Bioinformatics. 2014;

818 96. Kim D, Langmead B, Salzberg SL. HISAT: A fast spliced aligner with low memory
819 requirements. Nat Methods. 2015;

820 97. Trapnell C, Williams BA, Pertea G, Mortazavi A, Kwan G, Van Baren MJ, et al.
821 Transcript assembly and quantification by RNA-Seq reveals unannotated transcripts
822 and isoform switching during cell differentiation. Nat Biotechnol. 2010;

823 98. Trapnell C, Hendrickson DG, Sauvageau M, Goff L, Rinn JL, Pachter L. Differential
824 analysis of gene regulation at transcript resolution with RNA-seq. Nat Biotechnol.
825 2013;

826 99. Grohme MA, Schloissnig S, Rozanski A, Pippel M, Young GR, Winkler S, et al. The
827 genome of Schmidtea mediterranea and the evolution of core cellular mechanisms.
828 Nature. 2018;

829 100. Mootha VK, Lindgren CM, Eriksson KF, Subramanian A, Sihag S, Lehar J, et al.
830 PGC-1α-responsive genes involved in oxidative phosphorylation are coordinately
831 downregulated in human diabetes. Nat Genet. 2003;

101. Subramanian A, Tamayo P, Mootha VK, Mukherjee S, Ebert BL, Gillette MA, et al. Gene set enrichment analysis: A knowledge-based approach for interpreting genome-wide expression profiles. Proc Natl Acad Sci U S A. 2005;

102. Wickham H. ggplot2: elegant graphics for data analysis. ht tp. had. co. nz/ggplot2/book . Springer; 2009;

103. Goff LA, Trapnell C, Kelley D. CummeRbund: visualization and exploration of Cufflinks high-throughput sequencing data. R Packag version. 2012;

104. Ross KG, Molinaro AM, Romero C, Dockter B, Cable KL, Gonzalez K, et al. SoxB1 Activity Regulates Sensory Neuron Regeneration, Maintenance, and Function in Planarians. Dev Cell. 2018;

105. Butler A, Hoffman P, Smibert P, Papalexi E, Satija R. Integrating single-cell transcriptomic data across different conditions, technologies, and species. Nat Biotechnol. 2018;

106. Stuart T, Butler A, Hoffman P, Hafemeister C, Papalexi E, Mauck WM, et al. Comprehensive Integration of Single-Cell Data. Cell. 2019;

FIGURE LEGENDS

Figure 1. DDX24 is necessary for anterior regeneration in planarians.

(a) Dark-field images of control and *ddx24* KD tails regenerating head at 7th-day post-amputation. Eyespots are lost in absence of DDX24 (red arrows) (n > 100, 100% penetrant phenotype. Scale bar: 200 µm)

(**b)** Inability to regenerate eyes in *ddx24* KD corroborated by RNA-FISH for *Opsin* as well as immunostaining using anti-arrestin antibody. Either no eye structures were formed, or defective and rudimentary structures were formed. (Scale bar: 50 µm)

(c) Immunofluorescence using anti-Gα-q/11/14 antibody revealed defective cephalic ganglia regeneration in *ddx24* KD (Scale bar: 200 µm). Animals mostly regenerated an underdeveloped rudimentary brain as shown here. In extreme cases, no cephalic ganglia were observed. These observations were in agreement with RNA insitu for *pc2* as well as immunostaining using an anti-synapsin antibody, both of which also mark the cephalic ganglia (data not shown).

(**d)** RNA-insitu for *mat*, a bonafide gut marker. The anterior branch of the gut failed to regenerate in *ddx24* KD animals (red arrow). Also, no pharyngeal cavity (marked by asterisk *) was observed (Scale bar: 200 µm).

Figure 2. DDX24 protein was present in a subset of planarian body wall muscle fibers and X1 neoblasts.

(a) DDX24 immunofluorescence in intact planaria. The ventral surface from head and tail regions zoomed-in for greater clarity. The fibrous pattern, as seen here, is characteristic of planarian body wall muscle fibers. (NOTE: All the animals here are different) (Scale bar: 100 µm, n > 20)

(b) Amongst different muscle fiber subsets, DDX24 protein showed enriched expression in diagonal and longitudinal muscle fibers compared to circular muscle fiber. (Scale bar: 10 µm)

(c) DDX24 protein was expressed in a subset FACS sorted X1 neoblasts. (Scale bar: 50 µm (top) and 10 µm (bottom)).

Figure 3. *ddx24* mRNA was expressed by a subset of muscles, neoblasts, and neoblasts primed for muscle fate.

(a) Double-RNA-FISH confirmed that a subset of *ddx24* mRNA+ cells was also positive for *collagen*, a bonafide muscle marker. 65.8 ± 9.8% of *collagen*+ cells were also positive for *ddx24* whereas 46.7 ± 9.4% of *ddx24*+ cells were positive for *collagen*. (Scale bar: 50 µm)

(b) DDX24 protein was found to be enriched in longitudinal muscle fibers. *myoD* is the master transcription factor specifying this muscle subtype in planarians. 54.2 ± 10.7% of *myoD*+ cells also co-expressed *ddx24*. (Scale bar: 50 µm)

(c) A subset of *ddx24*+ cells are also *piwi1*+ neoblasts. 22.1 ± 4.6% of *piwi1*+ cells were also positive for *ddx24* whereas 18.8 ± 3.4% of *ddx24*+ cells were positive for *piwi1*. (Scale bar: 50µm)

(**d**) *ddx24* is expressed in a class of stem cells primed for muscle fate. We found that 36.5 ± 9.7% of PIWI1+ *ddx24*+ double-positive cells were positive for *collagen* too. (Scale bar: 20 µm)

(Note: The actual number of cells counted in each case is mentioned within the figure, with colour code. Every quantification percentage mentioned here was calculated in the entire volume specified by the red box on the adjacent planarian cartoon. 6 animals were used for quantification, except in (d) where 4 animals were used)

Figure 4. Loss of DDX24 leads to a defect in muscle fiber organization and integrity.

6G10 immunostaining revealed the loss of muscle fiber organization and their integrity in *ddx24* RNAi animals. Indentation and fracture in muscle fiber organization were observed on both the dorsal as-well-as on the ventral surface. Dark-field images and Hoechst staining revealed that there was otherwise no overall indentation or hole or lesion on these animals. This novel phenotype was restricted only to the muscle compartment. (Scale bar: 50 µm) (7-day post regenerating tail fragments)

Figure 5. Anterior pole cells express *ddx24* and the loss of DDX24 leads to defective anterior pole re-establishment during regeneration.

(a) The anterior pole (marked here by *zicA-foxD* expression), are specialized *collagen*+ muscle cells that are essential for head regeneration and patterning of anterior tissues. 79.9± 9.5% of *zicA-foxD*+ cells in intact planarians co-expressed *ddx24* at the head tip. (Scale bar: 20 µm, counting performed on 6 animals)

(b) Loss of DDX24 eliminated *foxD* and *zicA* expression at the head tip in 72 hpa tail fragments regenerating head.

(c) By 24 hpa, wound-induced *wnt1* expression reduces at the anterior blastema in control animals whereas higher number *wnt1*+ cells are still observed in *ddx24* KD animals. (Scale bar: 100 µm)

(d) Partial rescue of the eye-less *ddx24* RNAi phenotype by *β-catenin-1* RNAi in tail-fragments regenerating head (10-day post amputation animals). (Scale bar: 200 µm)

Figure 6: Loss of DDX24 leads to defective 28S ribosomal RNA processing and ribosome assembly.

(a) Gene ontology for pathways and processes up-regulated in d*dx24* KD indicated that the expression of many genes associated with rRNA processing was affected in *ddx24* knockdown.

(b) qRT-PCR for 18S rRNA, 28S rRNA, and *ddx24* transcript levels from 3DPA tail fragments from control and *ddx24* KD animals. All experiments were performed thrice. Mean ± SD indicated. Unpaired t-test was used to calculate statistical significance. Actin was used for normalization. (** implies p-value < 0.01)

(c) Polysome profiling on 3DPA tail fragments from control and *ddx24* KD animals. In absence of DDX24, a reduction in the 80S ribosome peak was observed.

Figure 1 (Supplementary)

(a) Multiple sequence alignment for DDX24 from different species. We found SMED-DDX24, like DDX24 from other species, contains the motifs conserved across DEAD-box helicases.

(b) Scheme and timeline of *ddx24* RNAi.

(c) Efficiency of *ddx24* RNAi was determined by RNA-Seq. RNA was extracted on the 3rd day-post-amputation.

(d) *ddx24* RNAi was specific. Even though planarians contain many DEAD Box Helicases, RNAi against *ddx24* was specific since transcript levels of *ddx24* alone got reduced.

(e) Defective pharynx regeneration in *ddx24* KD animals. 6G10, which also marks pharyngeal muscle, was used to probe defective pharynx regeneration. (Scale bar: 200 µm)

(f) Loss of DDX24 leads to an overall loss of regeneration in planarians. Head, trunk, and tail, all failed to regenerate eyespots and/or tails. For example, head fragments regenerating a tail failed to form the posterior gut branches **(g).**

Figure 2 (Supplementary)

(a) Western blot using anti-DDX24 antibody gave a band above 75KDa but lower than 90KDa.

(b, c) Validating the specificity of anti-DDX24 antibody by western blot ((b), N>5) and by immunostaining (c).

(d) In addition to being enriched in muscle fibers, we found other DDX24 protein+ cells in the post-pharyngeal space. Since we were unable to perform DDX24 immunostaining post-RNA-FISH, we couldn't confirm the identity of these cells.

Figure 3 (Supplementary)

(a, b) *ddx24* mRNA also co-localized with *bwm1* and *nkx1.1*. In addition to *collagen* and *myoD*, these two are also bonafide muscle markers in planarians. 63.4±7.6% and 21.3±7.8% *bwm1+* and *nkx1.1+* cells respectively were also positive for *ddx24*. (Scale bar: 50 µm, 3 animals were used for quantification)

(c) RNA-FISH for *ddx24*. Different regions highlighted- head tip, post-pharyngeal space, and cephalic ganglia. *ddx24* transcript was found to be enriched more on the ventral side of the animals as compared to the dorsal side. (scale bar: 20 µm) (**d)** *ddx24* RNA-FISH validation. (Scale bar: 100 µm)

(e) Single-cell RNA sequencing profile for *ddx24* across different tissue types (Fincher et al., 2018). Supplementary table S4, Fincher et al., 2018, also listed *ddx24* as a posterior muscle enriched transcript.

(f) Single-cell RNA sequencing profile for *ddx24* across different X1 neoblast clusters (Zeng et al., 2019). In addition to other lineages, both (e, f) suggested that *ddx24* was expressed in a subset of neoblasts and muscles, including specialized muscles are known as anterior-pole progenitor cells.

(g) *ddx24+* single cells from Fincher et al., 2018, were extracted and re-analysed for the co-expression of other transcripts, as described by Ross et al., 2018. We overlaid the expression of selected stem cell genes, muscle genes, and positional-control and patterning genes on the *ddx24+* single cells. This co-expression dataset helped us corroborate the veracity of our RNA-FISH imaging data.

Figure 4 (Supplementary)

(a) Some *ddx24* KD animals displayed muscle fiber indentation at the anterior tip. This region houses a group of specialized muscle cells called anterior pole cells which are

necessary for head regeneration as well as patterning of different anterior tissues. (Scale bar: 50 µm)

(b) *collagen* mRNA is a bonafide muscle marker in planarians. RNA-FISH for *collagen* suggested that *ddx24* KD animals have similar collagen levels w.r.t. control fragments. This implied that neoblasts differentiated into *collagen+* muscle cells but the muscle fibers somehow failed to organize themselves appropriately in absence of DDX24. (Scale bar: 200 µm)

(c) 3D movie showing 6G10 staining in control and *ddx24* KD animals. Muscle fiber rupture on both the dorsal as well as on the ventral surface can be seen here. Also, 6G10 stained *ddx24* KD animals weakly w.r.t control animals. All staining was performed on 7 DPA tail fragments.

(d) Disruption of muscle fiber architecture was also observed in 7 DPA *ddx24* KD head fragments regenerating tail. (Scale bar: 100 µm)

Although a subset of neoblasts was positive for DDX24 protein as well as for mRNA, loss of DDX24 did not affect neoblasts or their proliferation **(e, f, g, h)**. H3P makers proliferating neoblasts, *piwi1* mRNA is a pan-neoblast marker, whereas PIWI1 protein is present in all naïve neoblasts, primed neoblasts as well as their immediate early progeny. In addition, Log2FoldChange values for different neoblast associated transcripts (*tspan1*, *tgs1*, *dd_648*, *vasa1*, and *piwi1*) from RNA sequencing performed on 72 hpa tails suggested that their levels were comparable in *ddx24* KD animals w.r.t. controls.

(j) Log2FoldChange values for different progenitor transcripts indicated that DDX24 KD animals did not display differentiation defect. RNA-Seq was performed in 3 DPA tail fragments. This data was further corroborated by RNA-FISH for collagen on 7 DPA animals. collagen differentiation from *piwi1+* neoblasts seemed unperturbed in *ddx24* KD animals (Figure 4-figure supplement 4b).

Figure 5 (Supplementary)

(a) *ddx24* was expressed at the 72 hpa head blastema region (area enclosed by white dashed lines). During this time, *ddx24* was also expressed by *zicA+foxD+* anterior pole progenitor cells in this region (yellow arrows) (Scale bar: 50 µm)**.**

(b) *notum* expression was also reduced at the pole region in a subset of *ddx24* KD animals by 72 hpa. In other animals, mis-expression of *notum* (white arrows) was observed. (Scale bar: 50 µm).

(c) Loss of DDX24 leads to a reduction in expression and/or mis-expression of different position-control genes and patterning genes required for bonafide head identity.

(d) We performed bulk RNA sequencing from 3DPA (72HPA) tail fragments regenerating the head. In addition to corroborating our staining above, we saw that expression of many other well-known genes essential for proper head regeneration and patterning were down-regulated in *ddx24* KD animals.

(e) Dayan Li et al., 2019, provided a comprehensive list of transcripts up-regulated in the head primordia by 3DPA (72 HPA). Comparing our transcriptome data with this paper gave us two sets of genes- (1) one set was down-regulated in *ddx24* KD and (2) the other set was up-regulated in *ddx24* KD. This further seemed to suggest that anterior pole determination was abnormal in absence of DDX24.

(f) PCG expression during tail regeneration in *ddx24* KD animals. Although expression of tail determinants/markers like *wntP2/wnt11-5* and *fz-4-1* weren't aberrant in absence of DDX24, the number of *wnt1+* cells at the tail tip was highly upregulated.

Figure 1

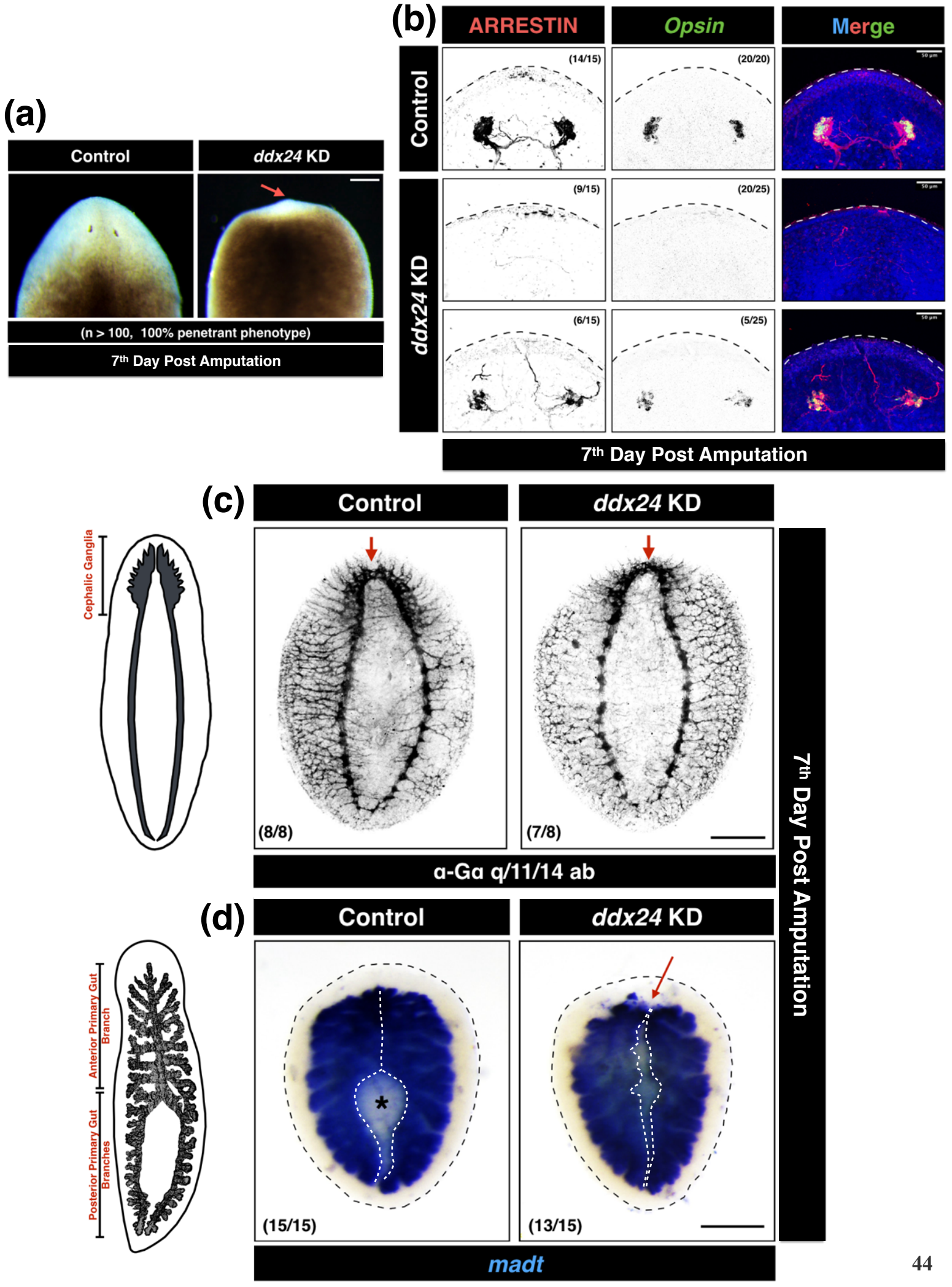

Figure 2

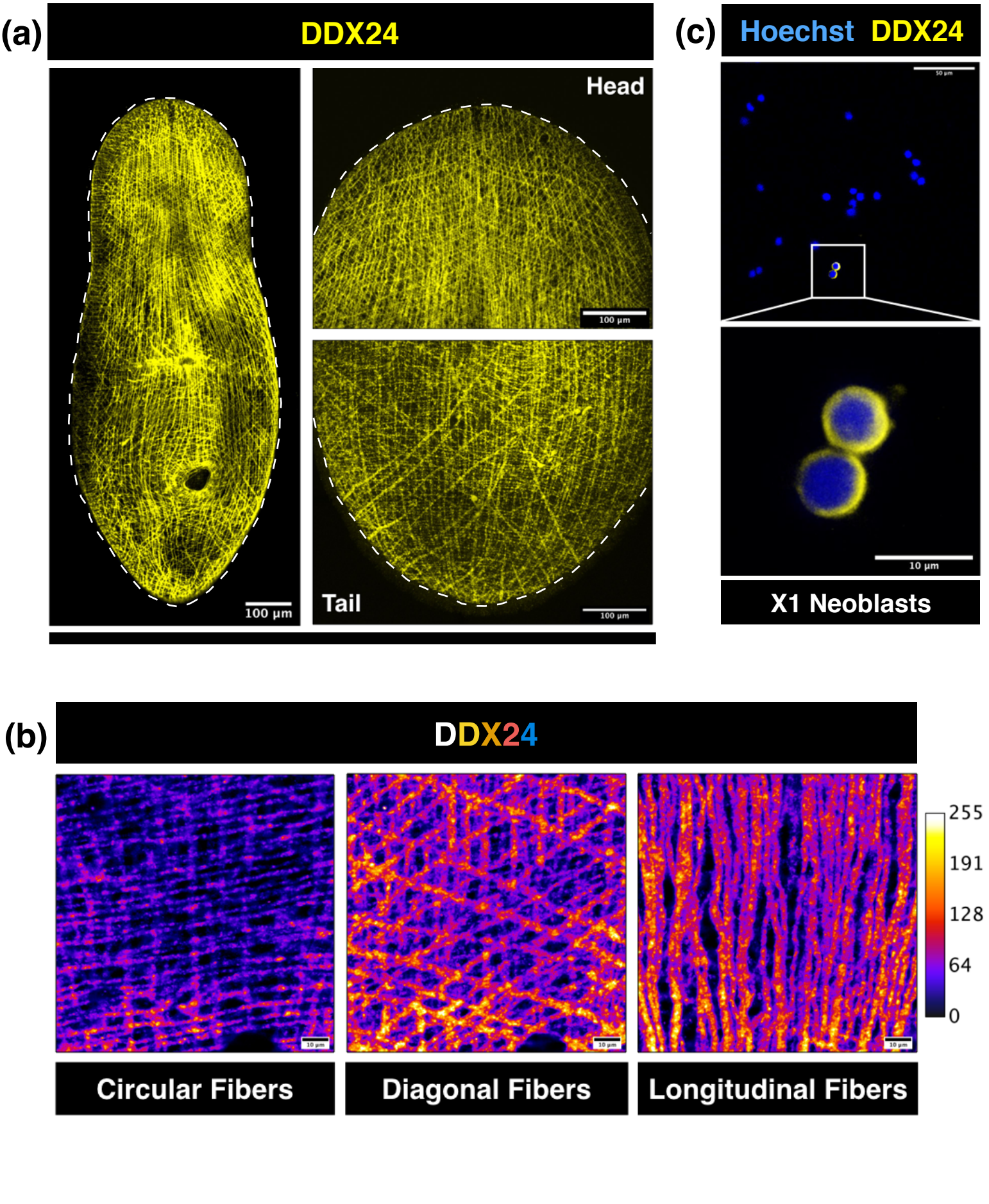

Figure 3

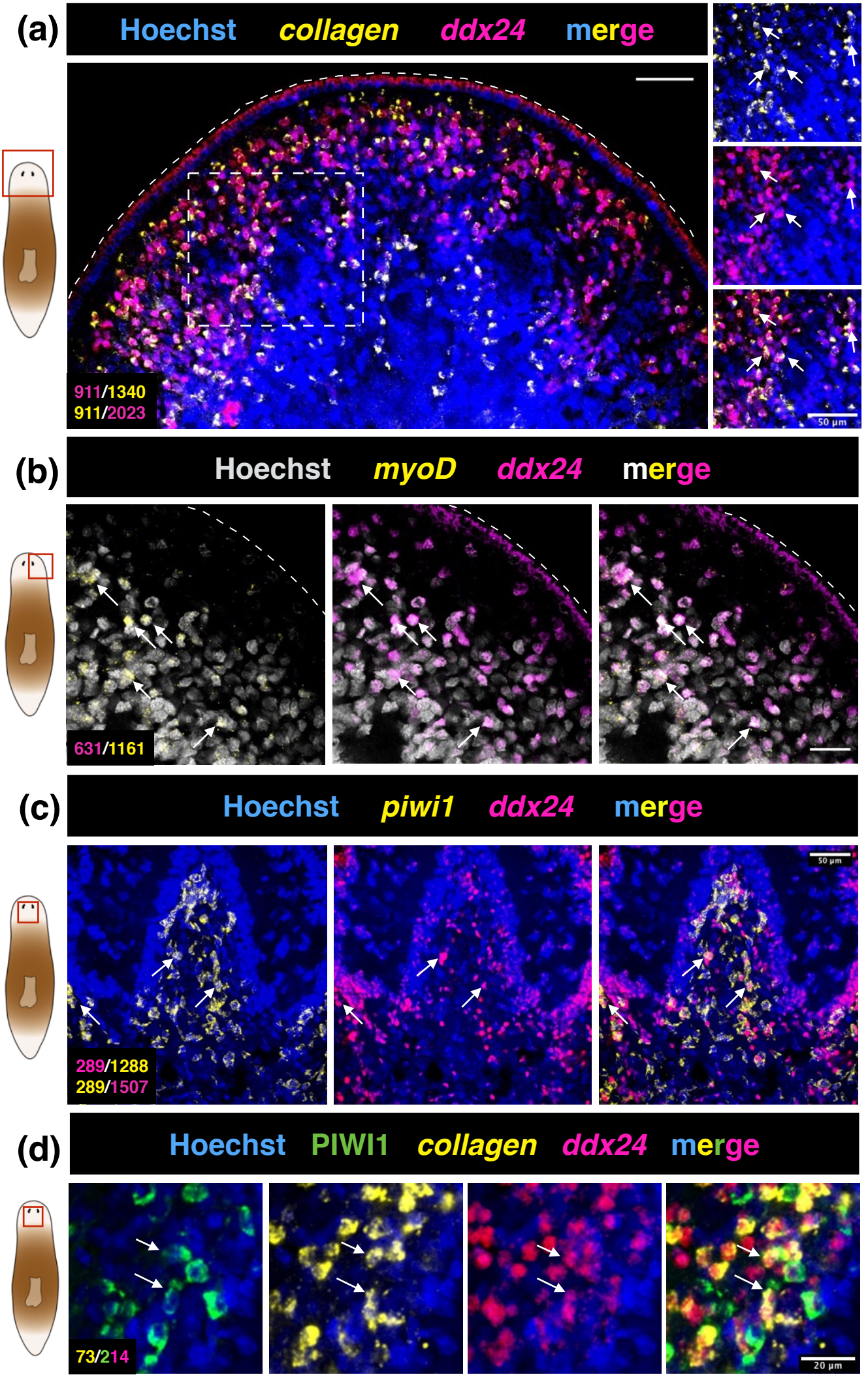

Figure 4

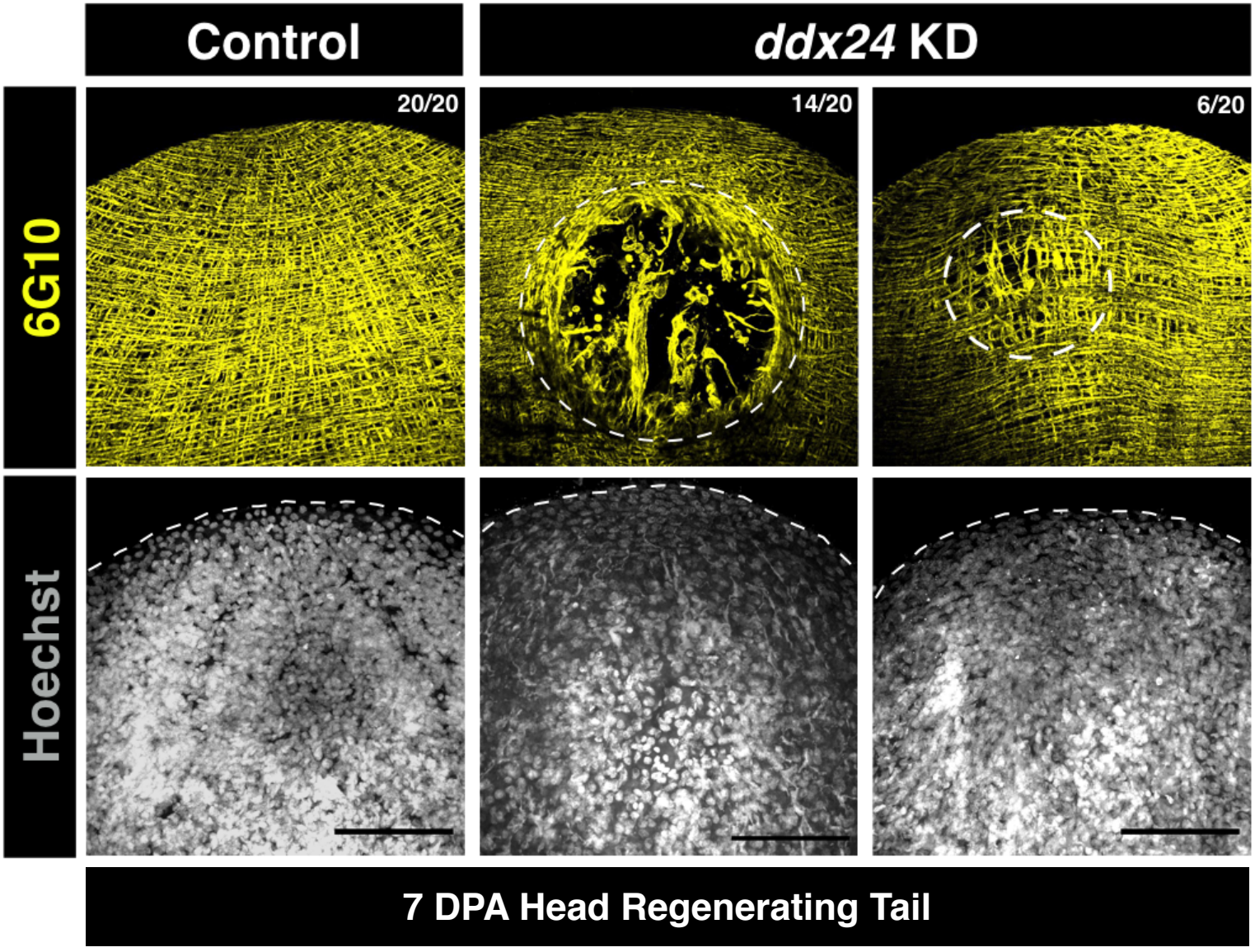

Figure 5

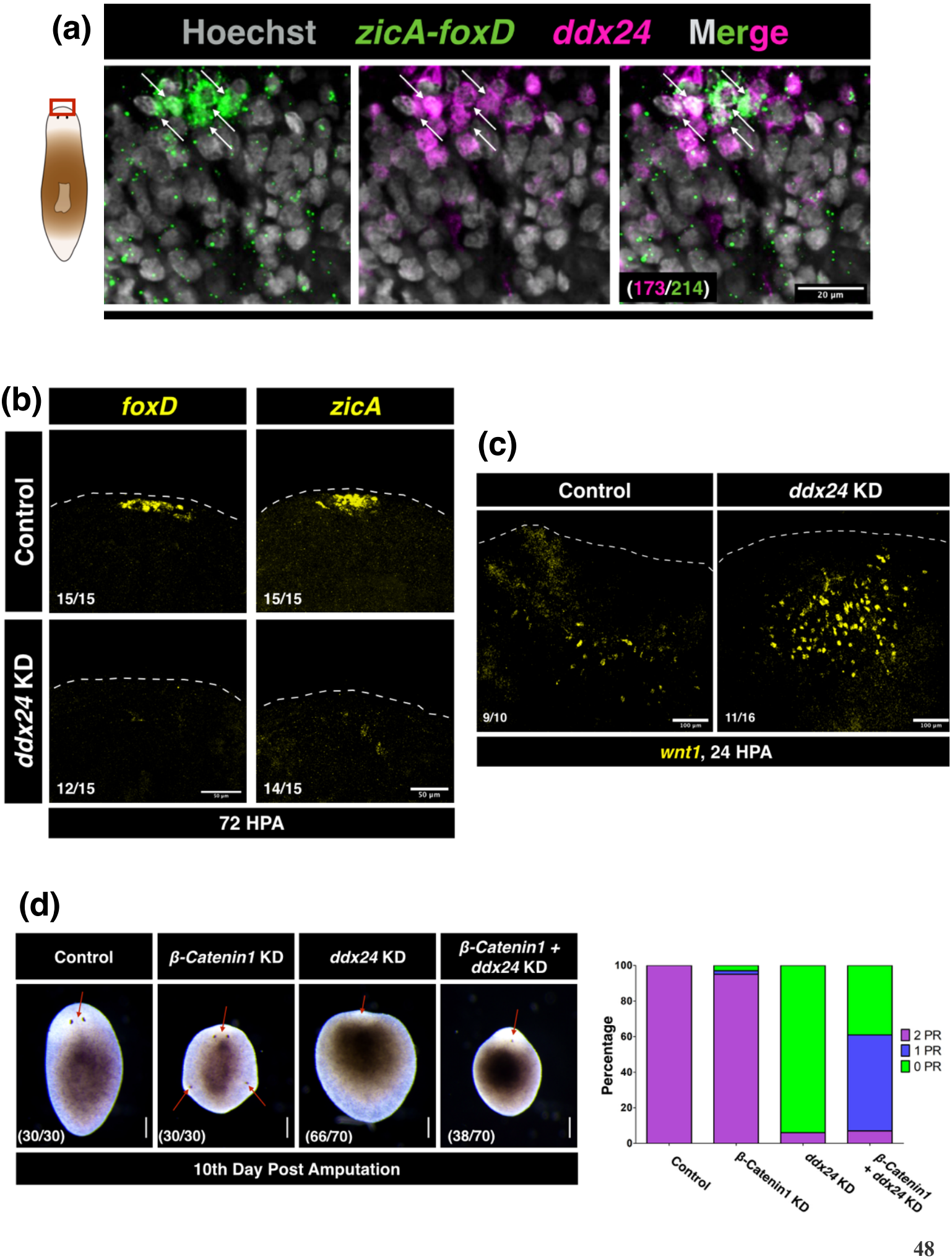

Figure 6

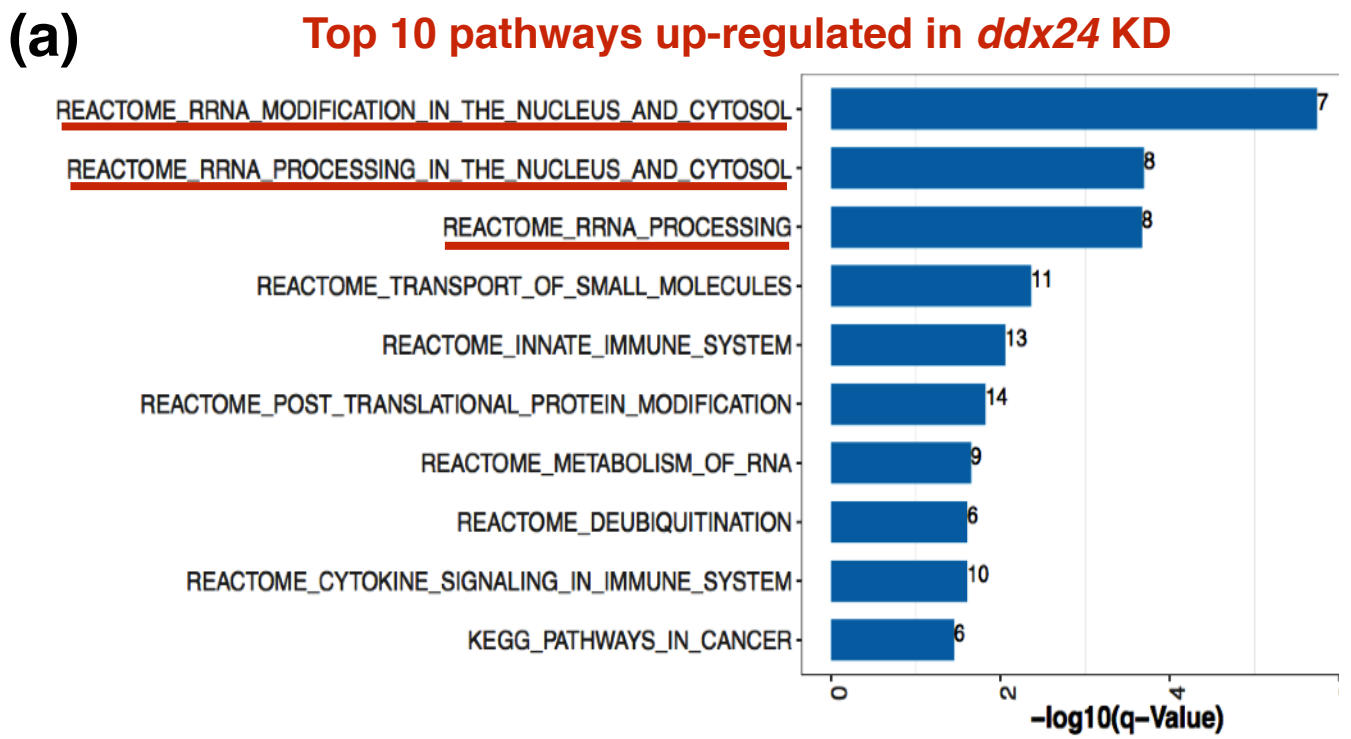

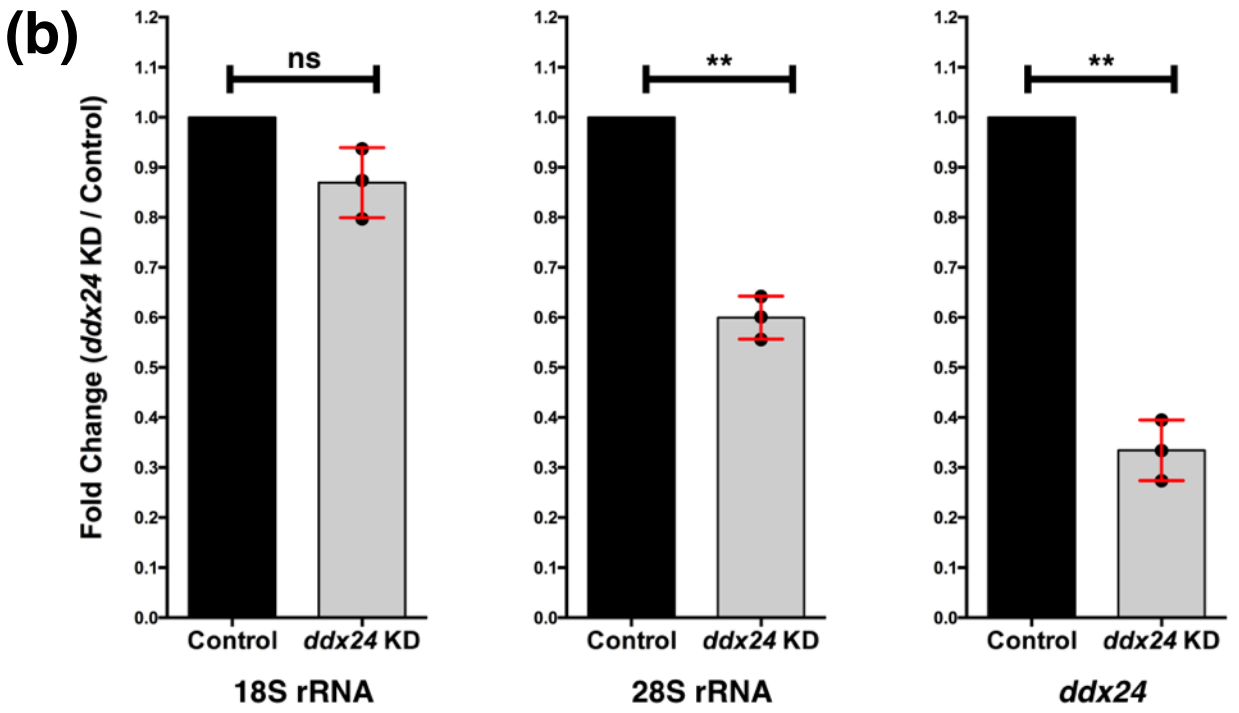

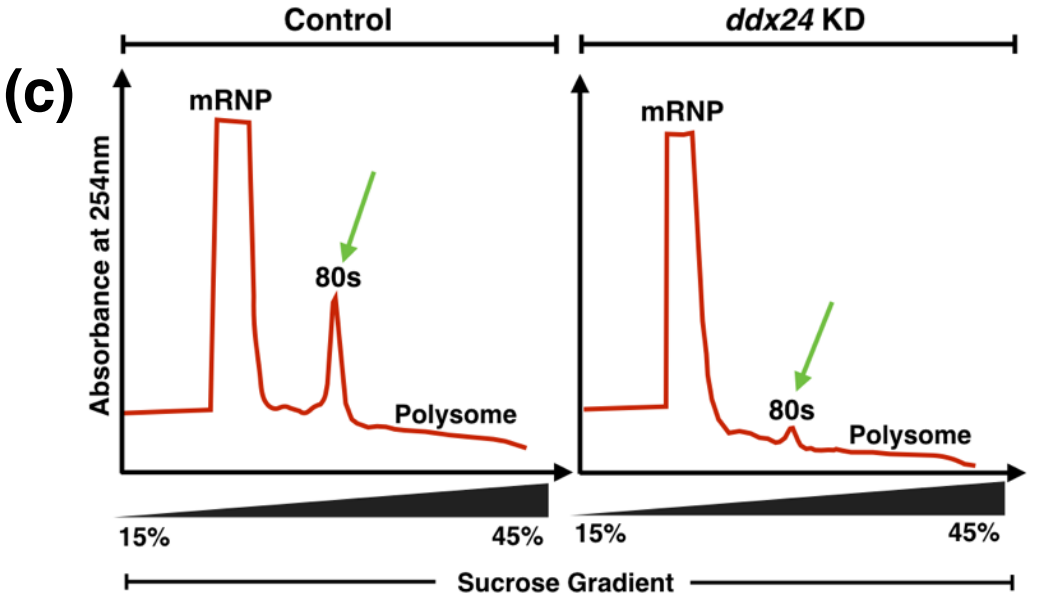

Figure 7 (Working Model)

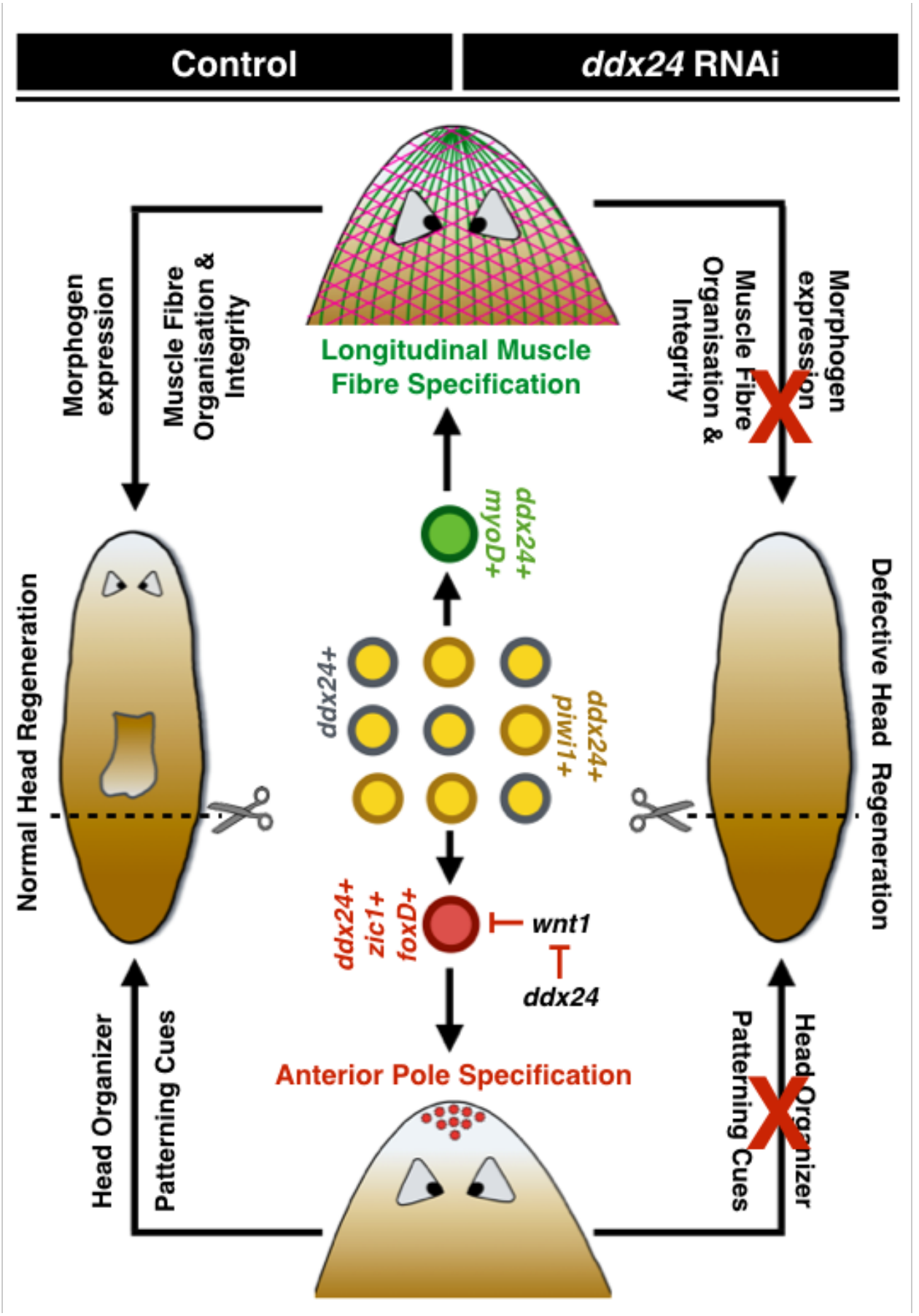

Figure 1 (Supplementary)

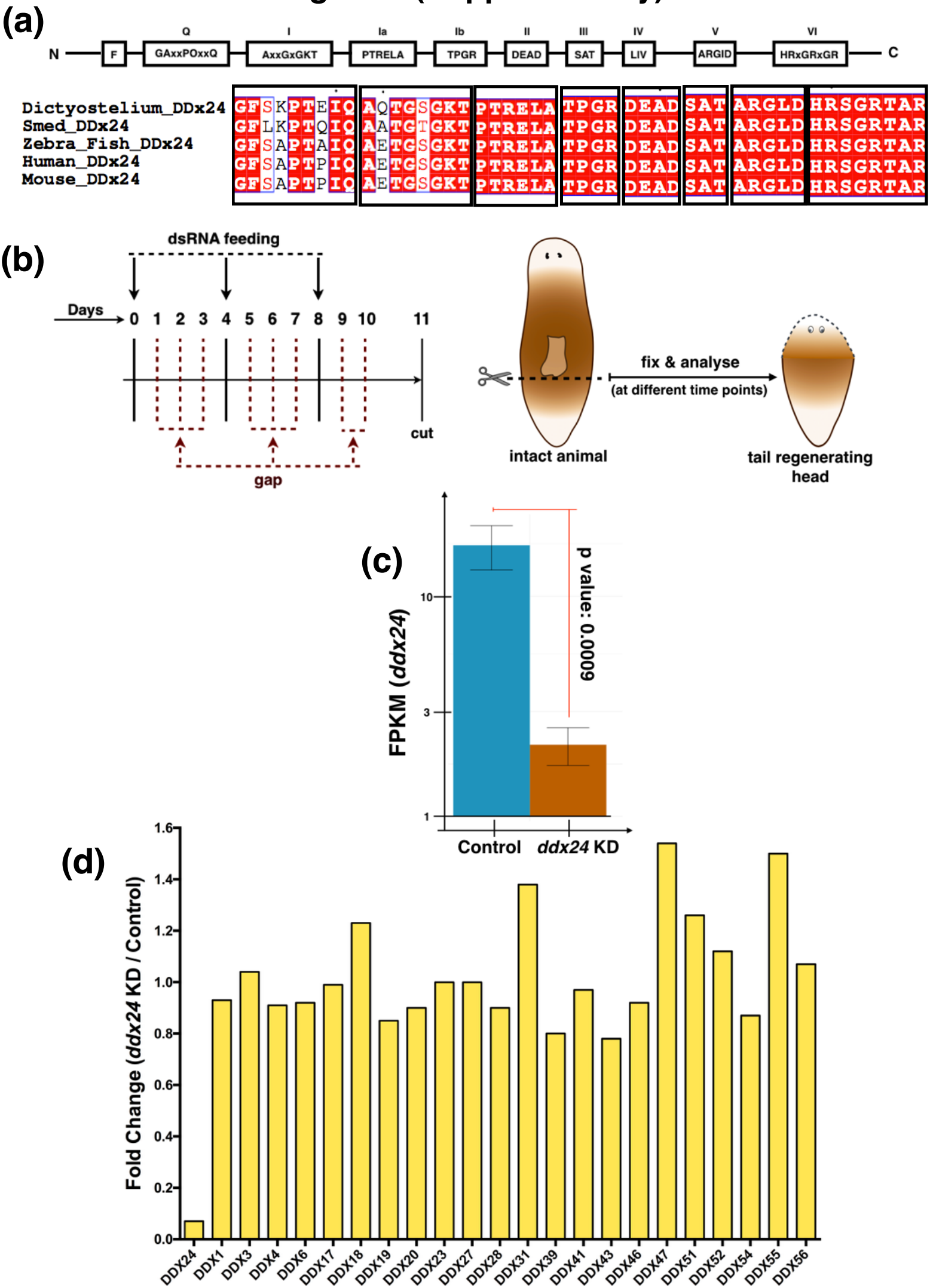

Figure 1 (Supplementary)

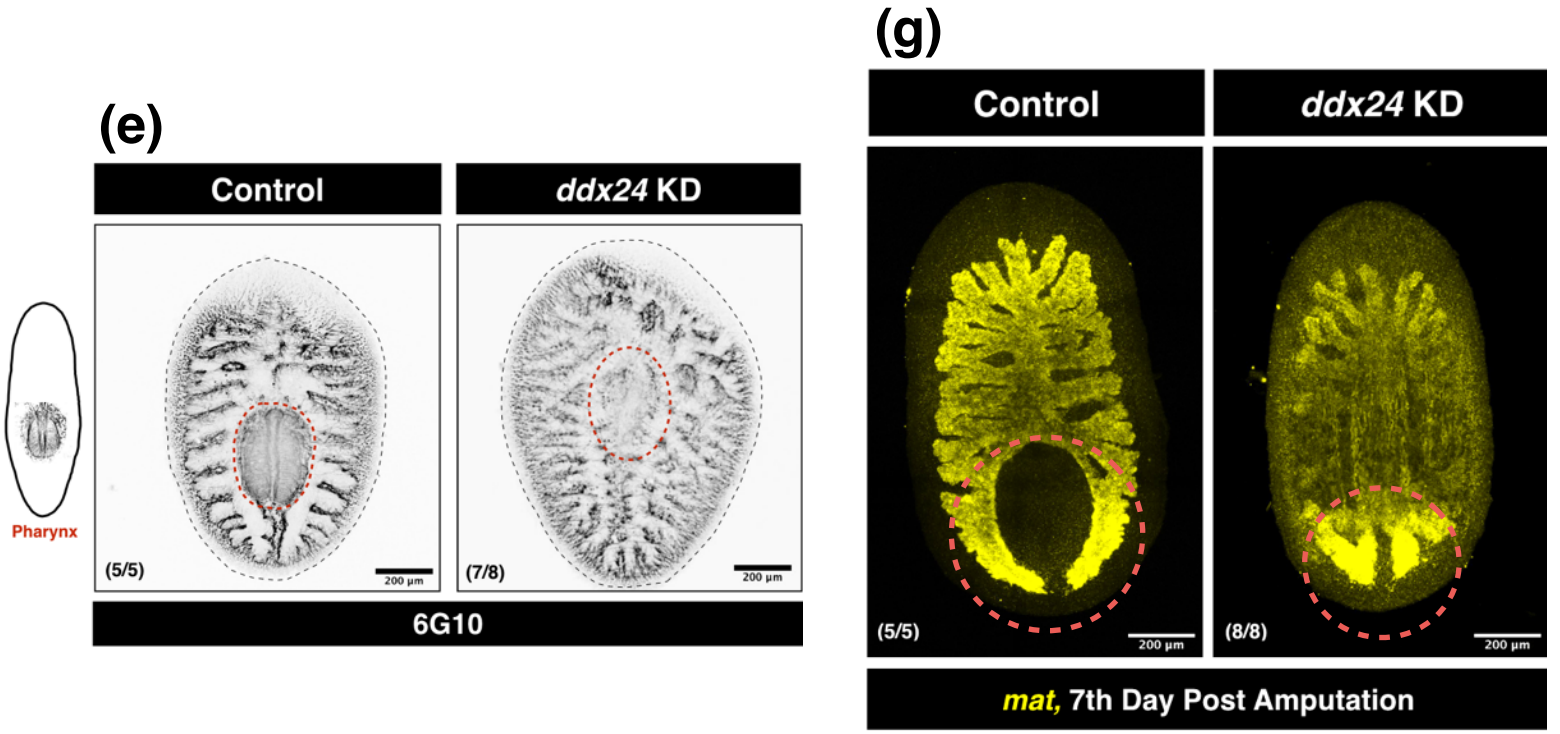

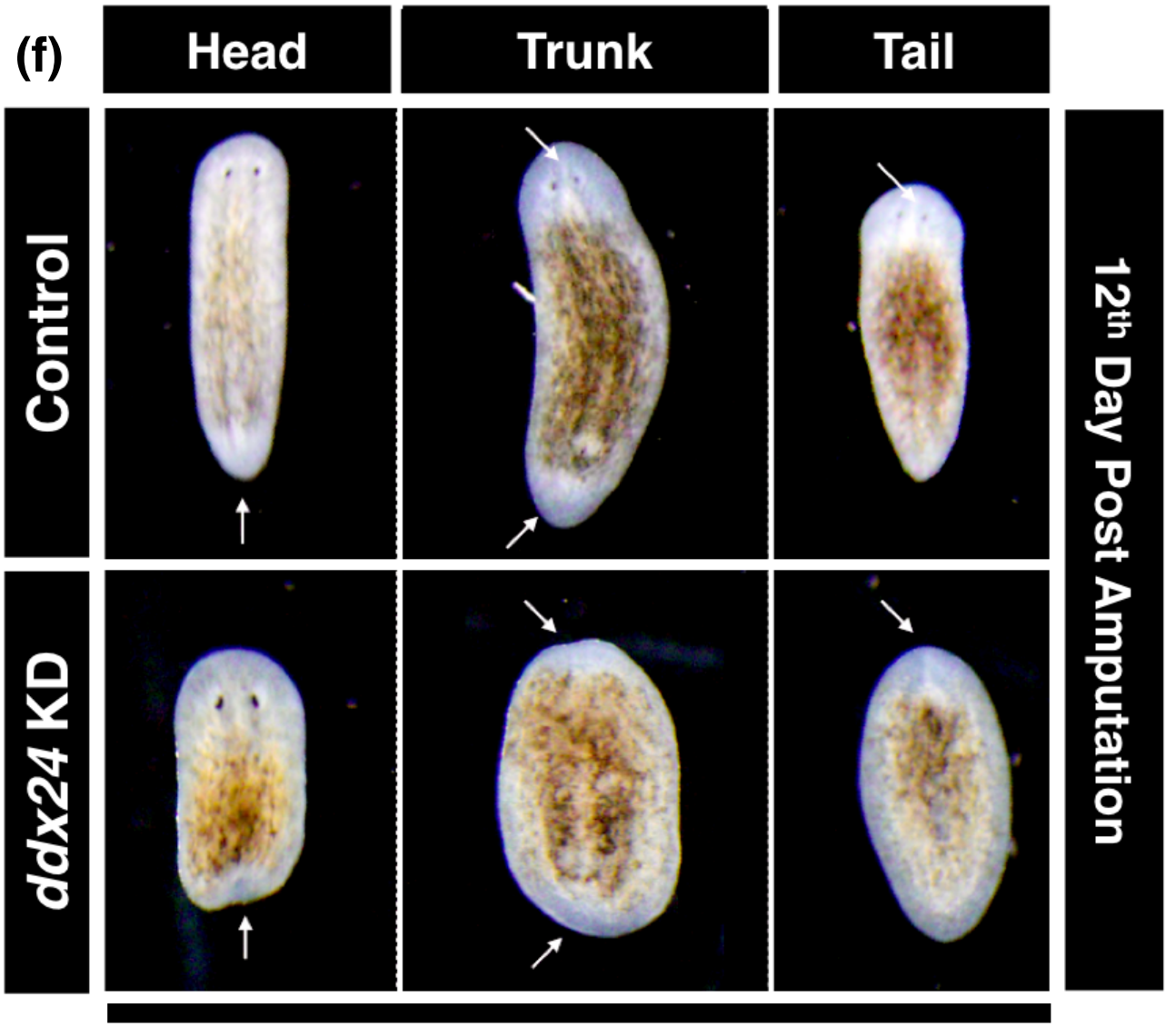

Figure 2 (Supplementary)

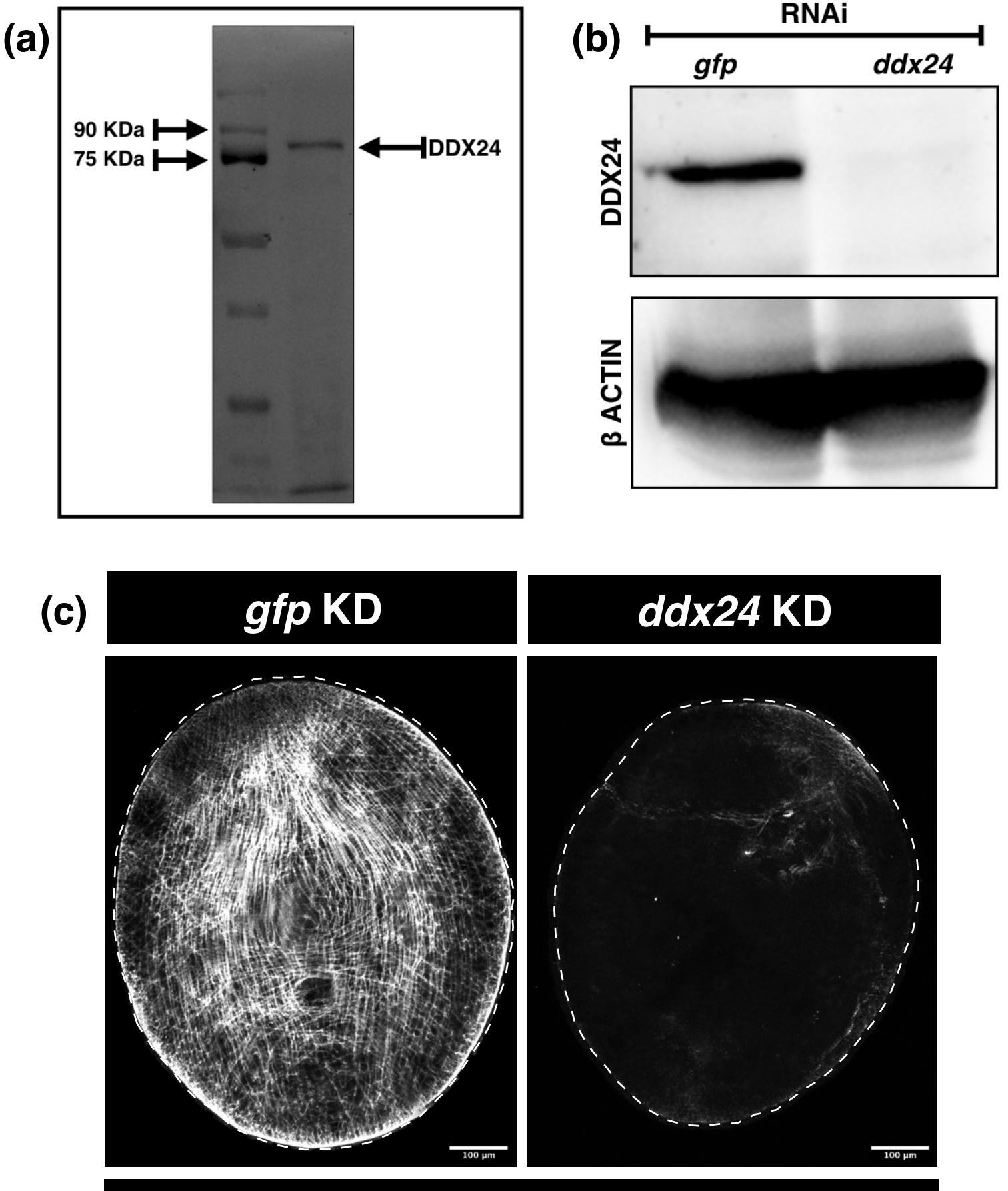

Figure 2 (Supplementary)

(d)

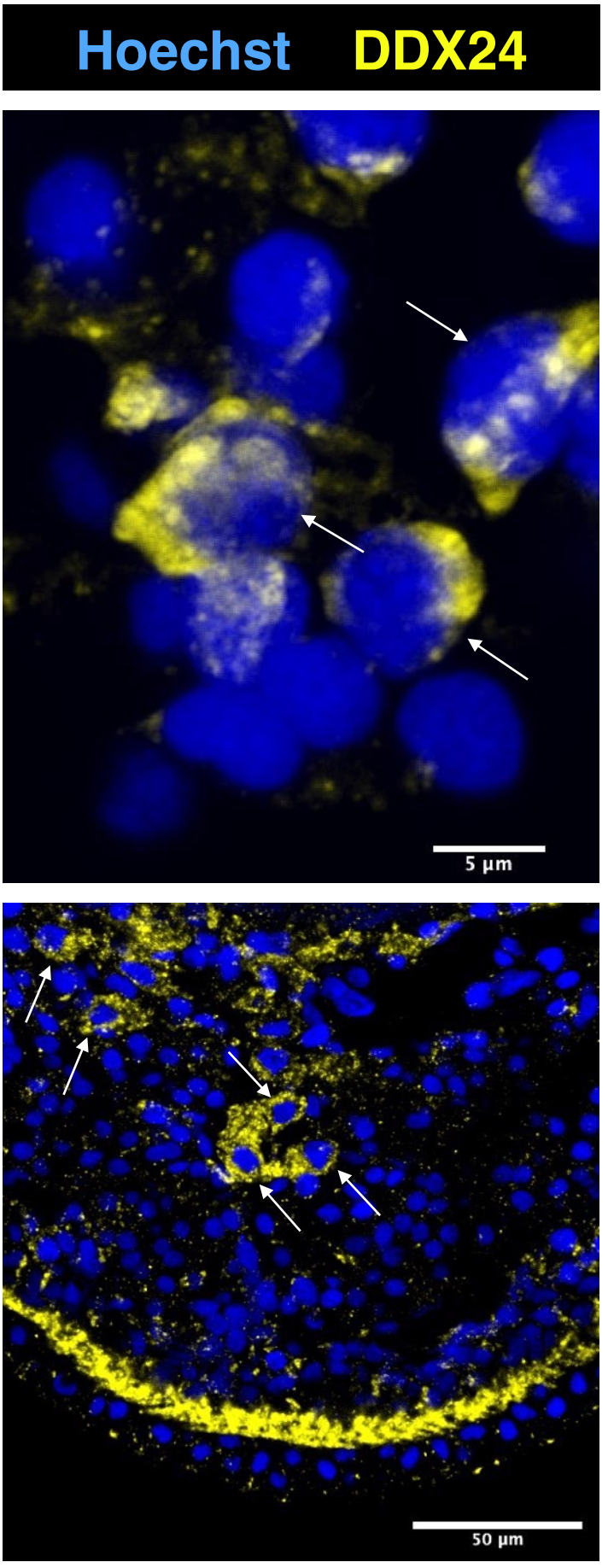

Figure 3 (Supplementary)

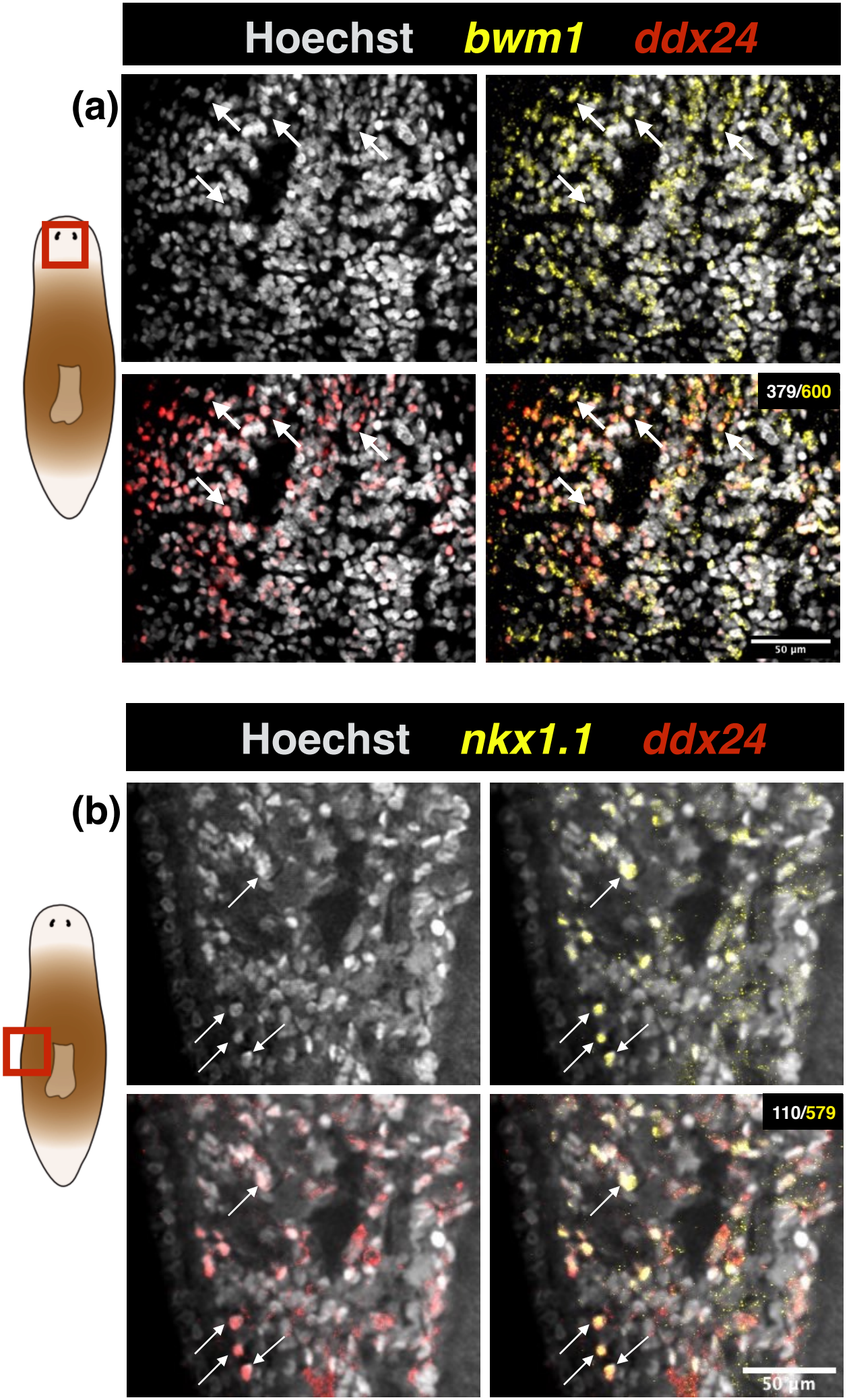

Figure 3 (Supplementary)

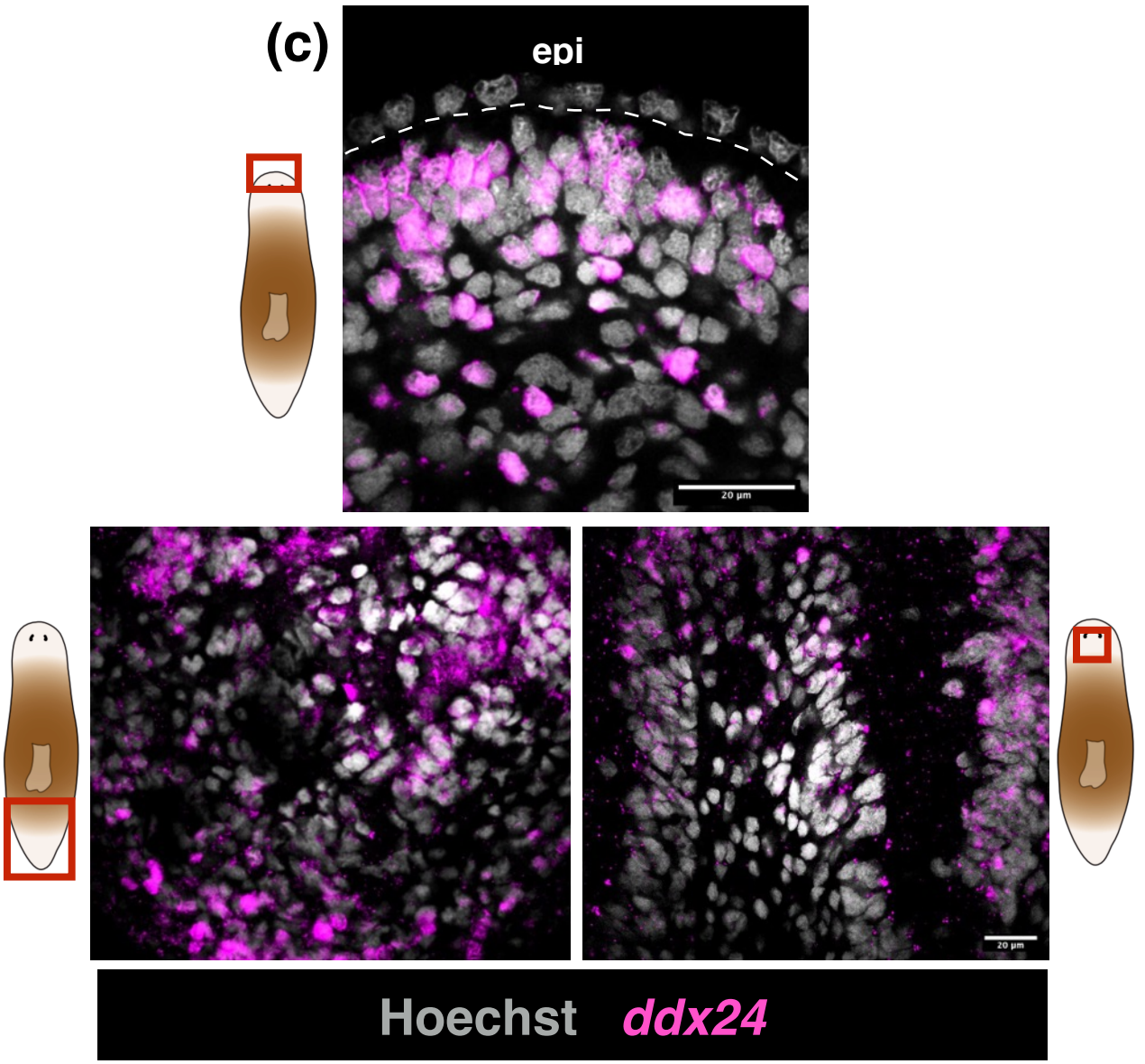

Figure 3 (Supplementary)

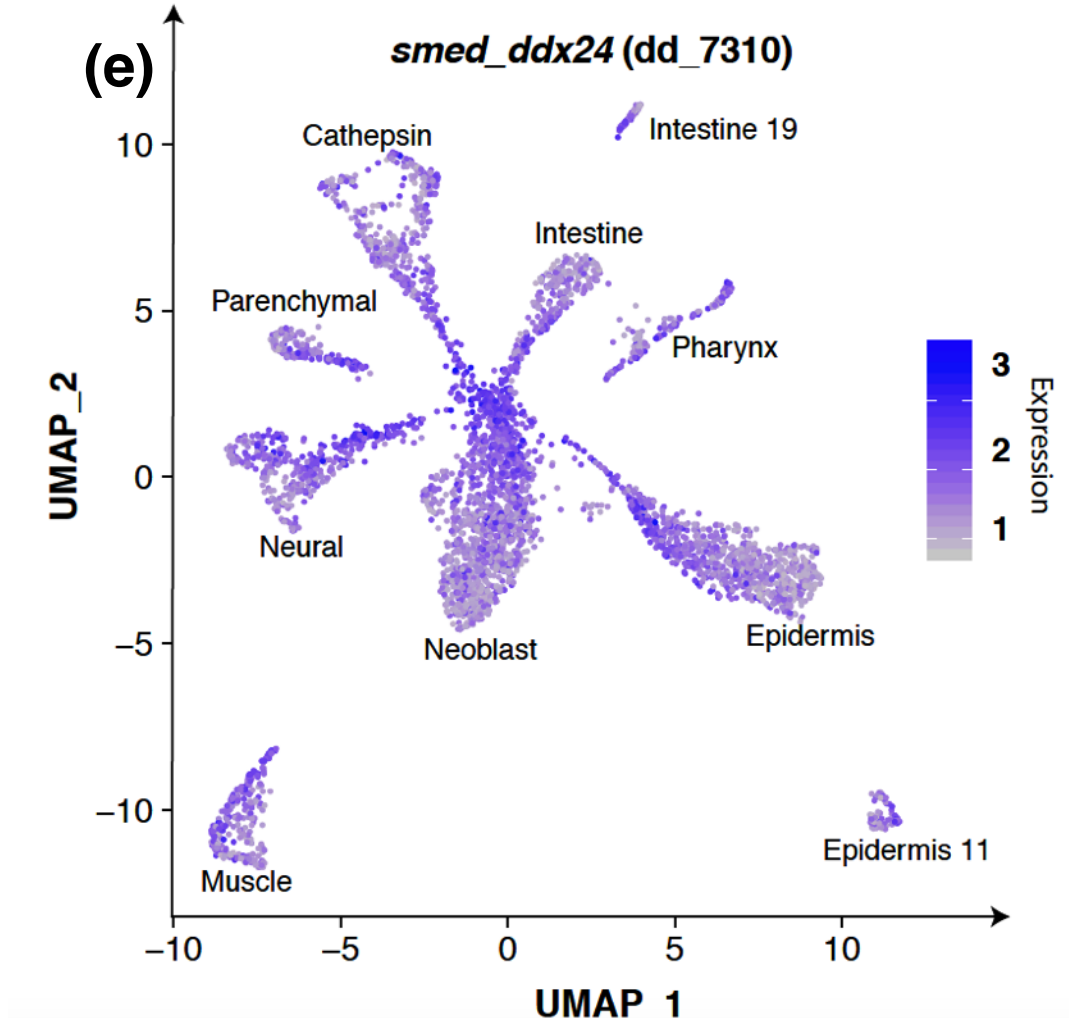

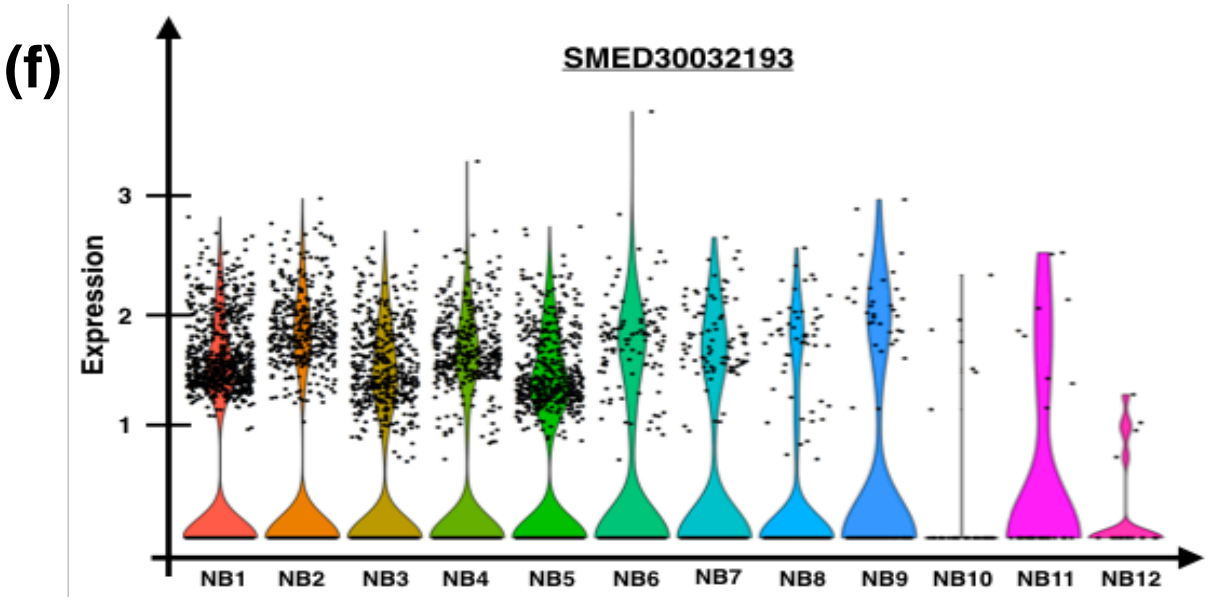

Identity

NB1: Epidermal Progenitor 2
NB2: cNeoblast
NB3: Epidermal Progenitor 1
NB4: Muscle Progenitor
NB5: Gut Progenitor
NB6: Anterior Pole Progenitor
NB7: Pharynx Progenitor 1
NB8: Pharynx Progenitor 2
NB9: Protonephridia Progenitor
NB10: Parapharyngeal
NB11: nu-neoblast
NB12: Gut precursor

Figure 3 (Supplementary)

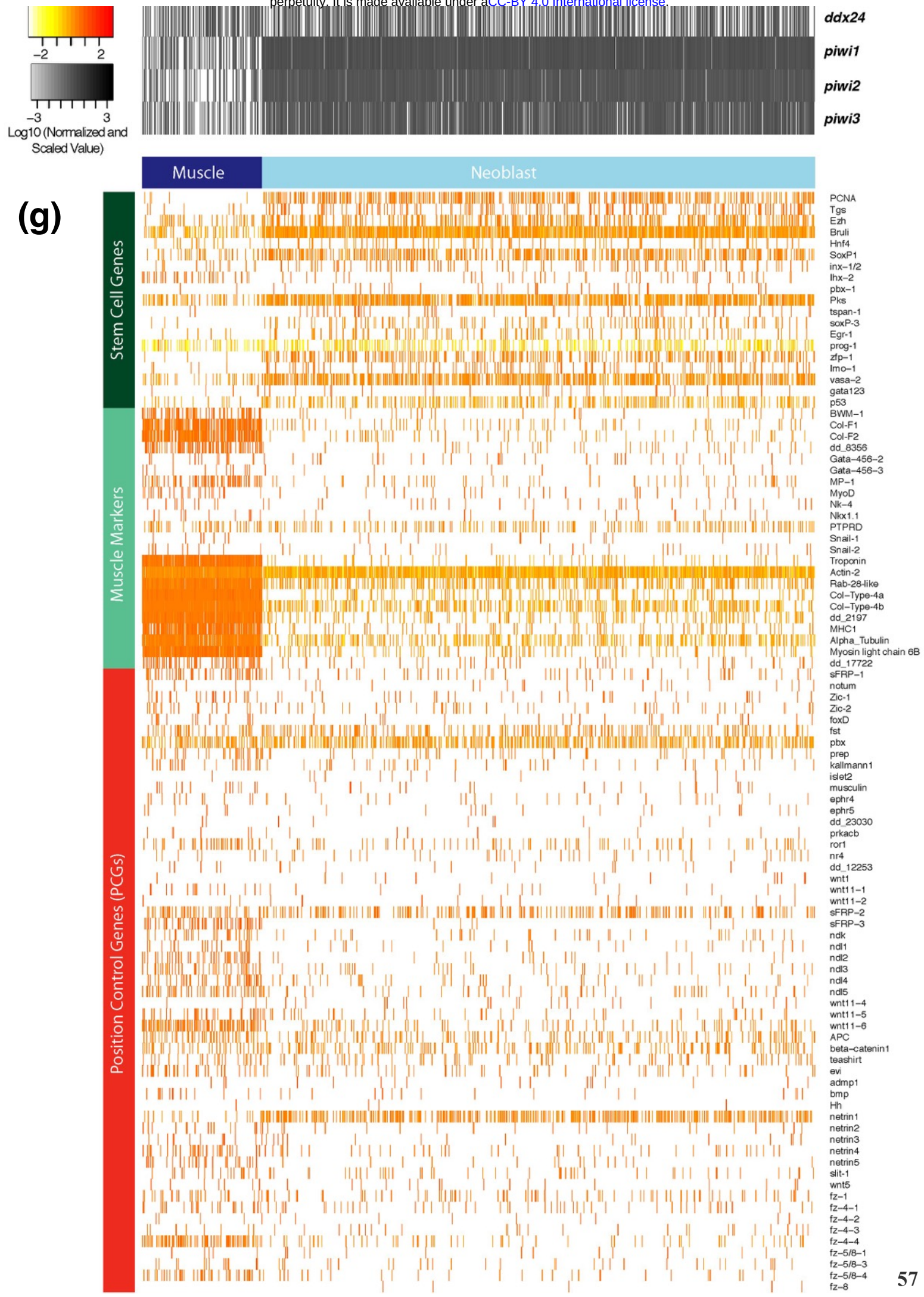

Figure 4 (Supplementary)

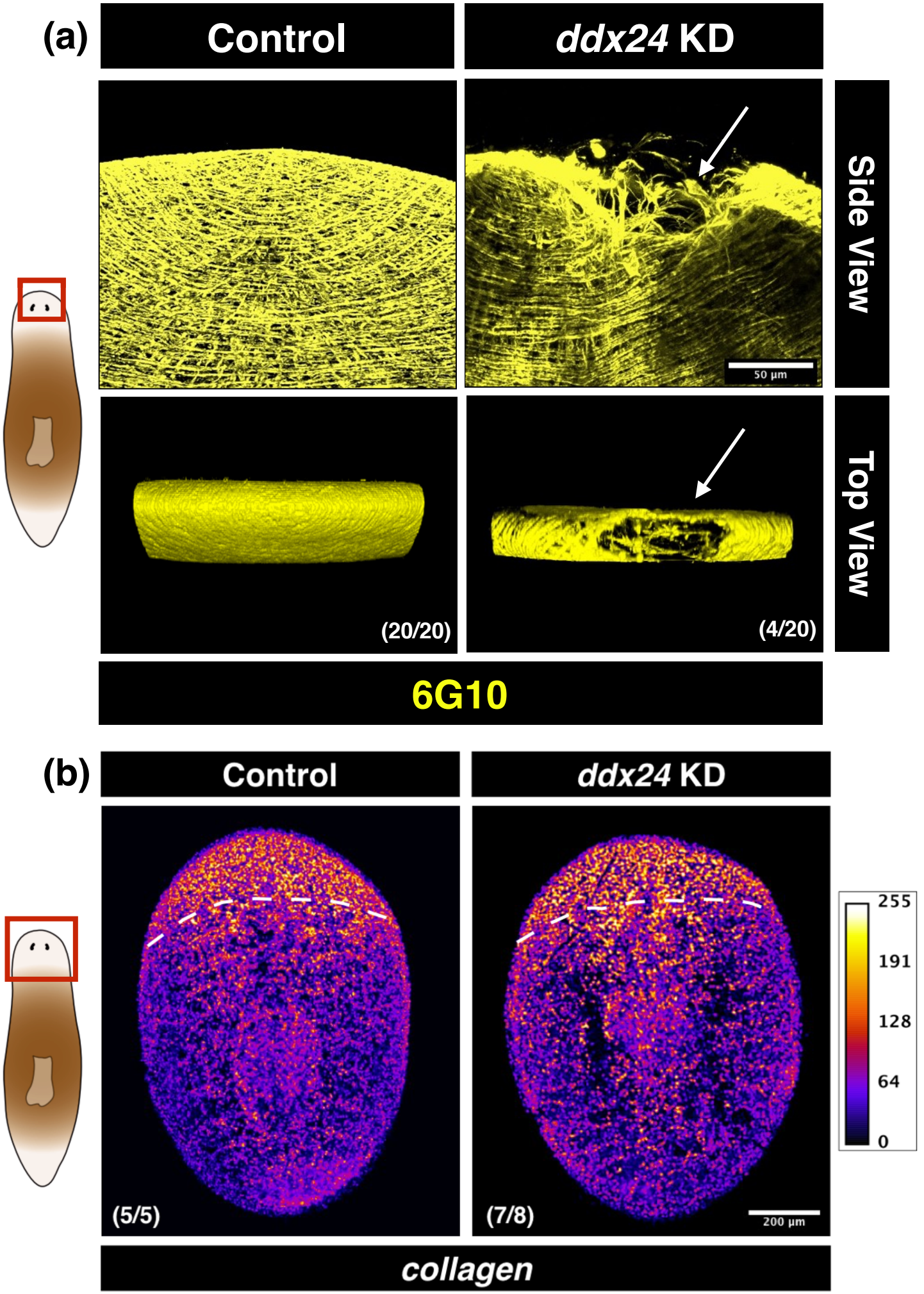

Figure 4 (supplementary)

(c)

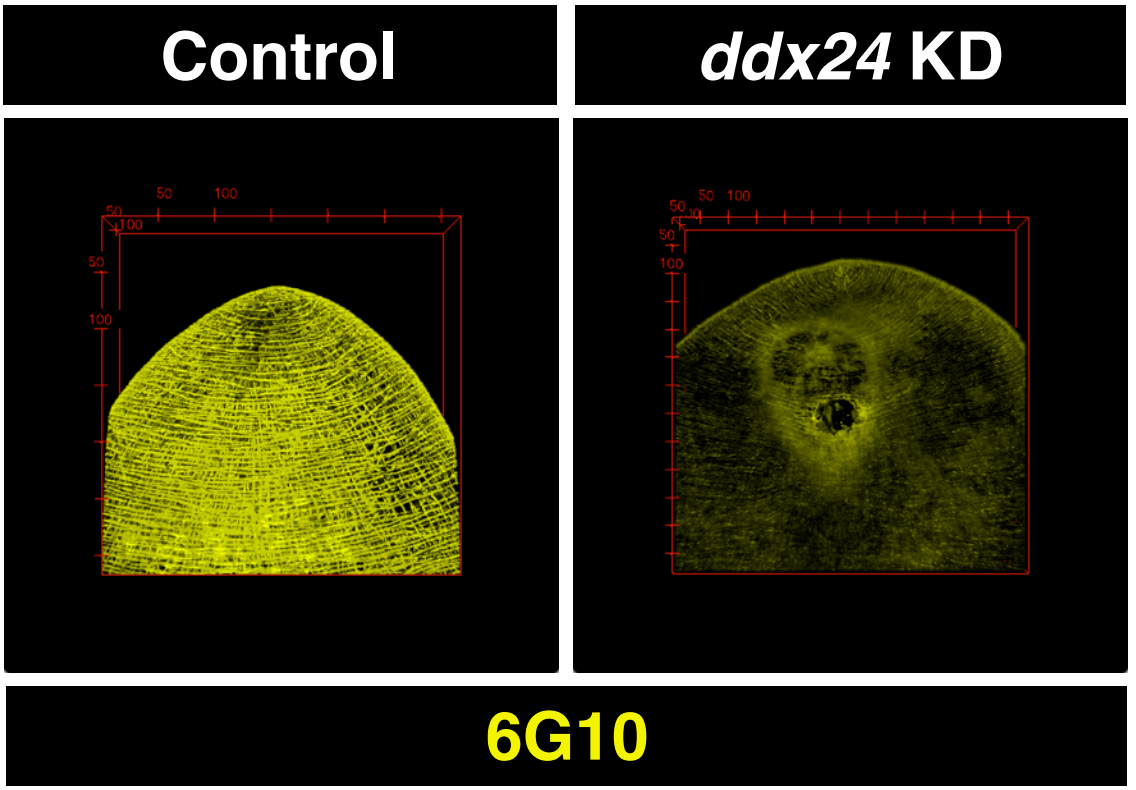

(d)

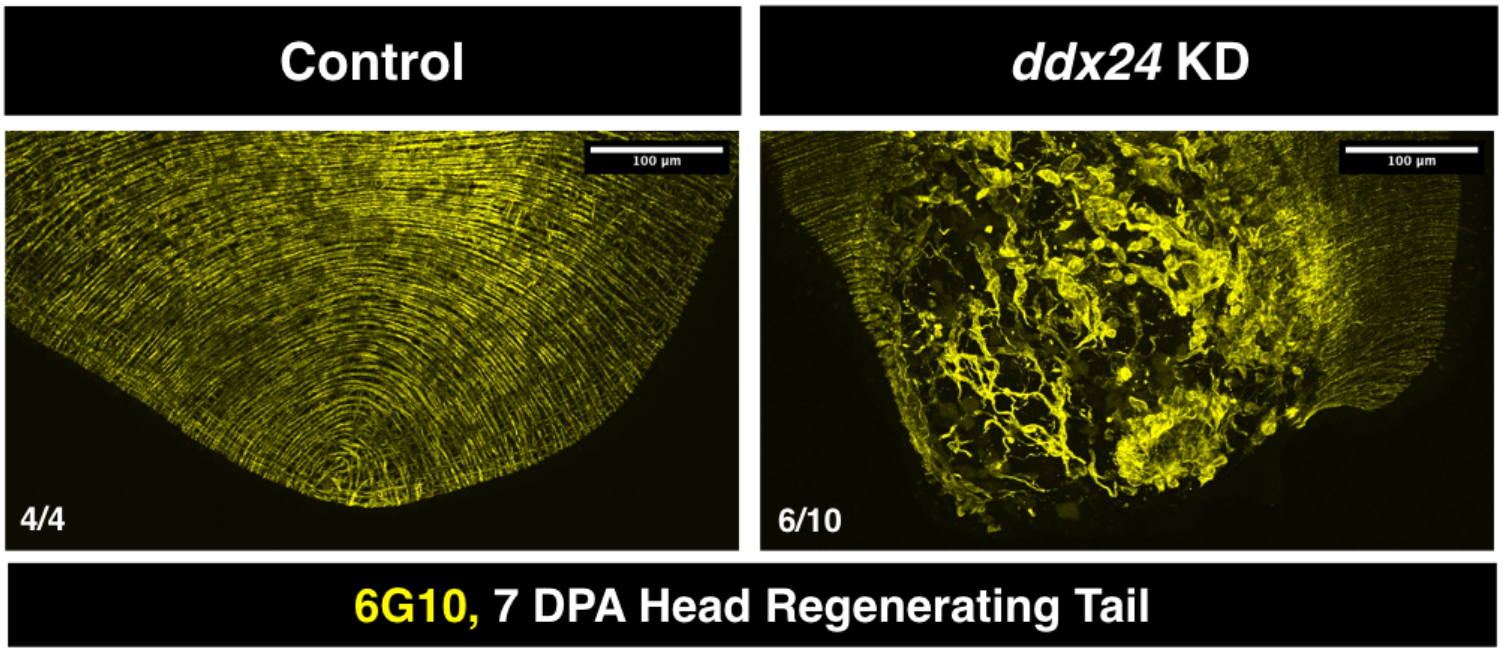

Figure 4 (Supplementary)

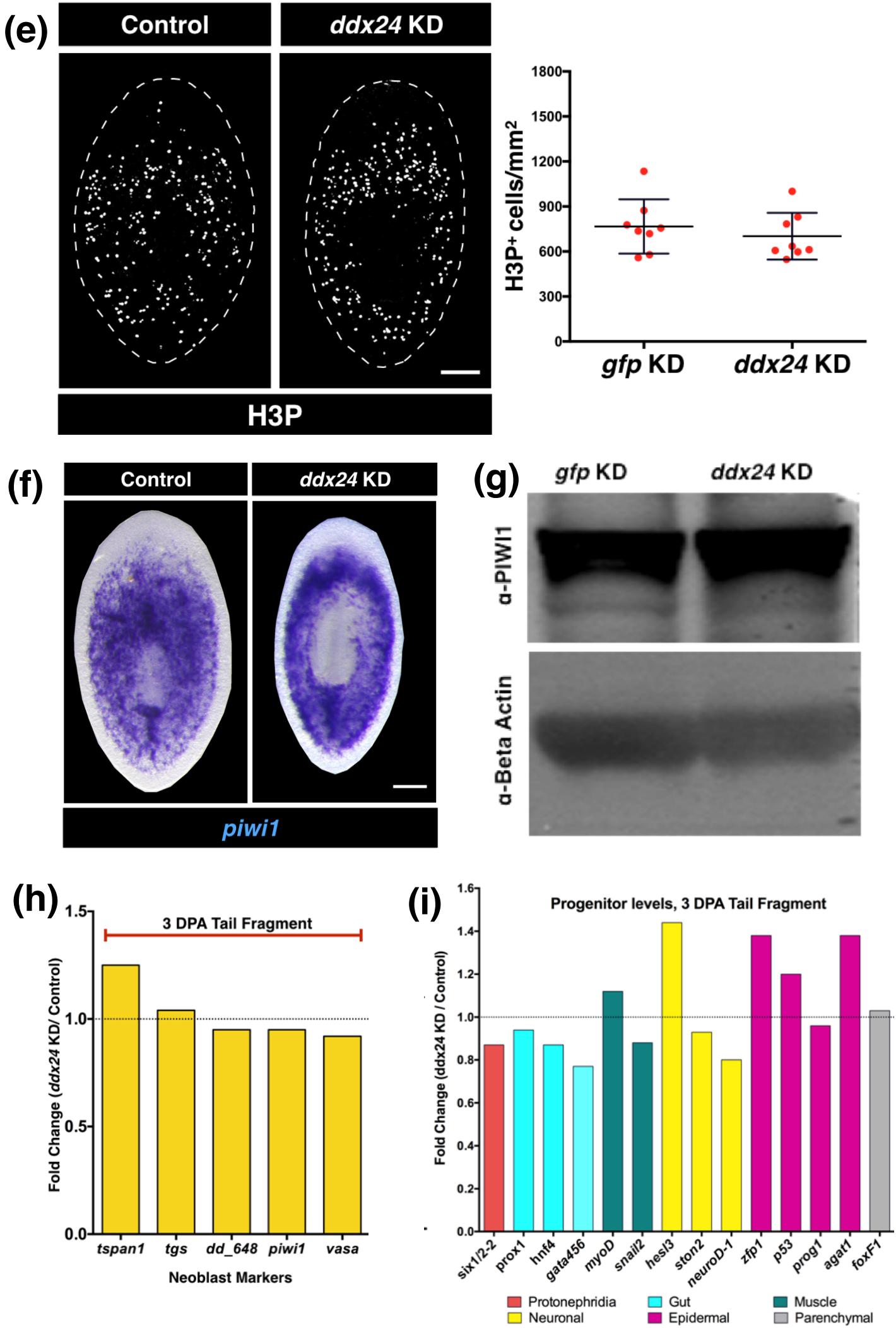

Figure 5 (Supplementary)

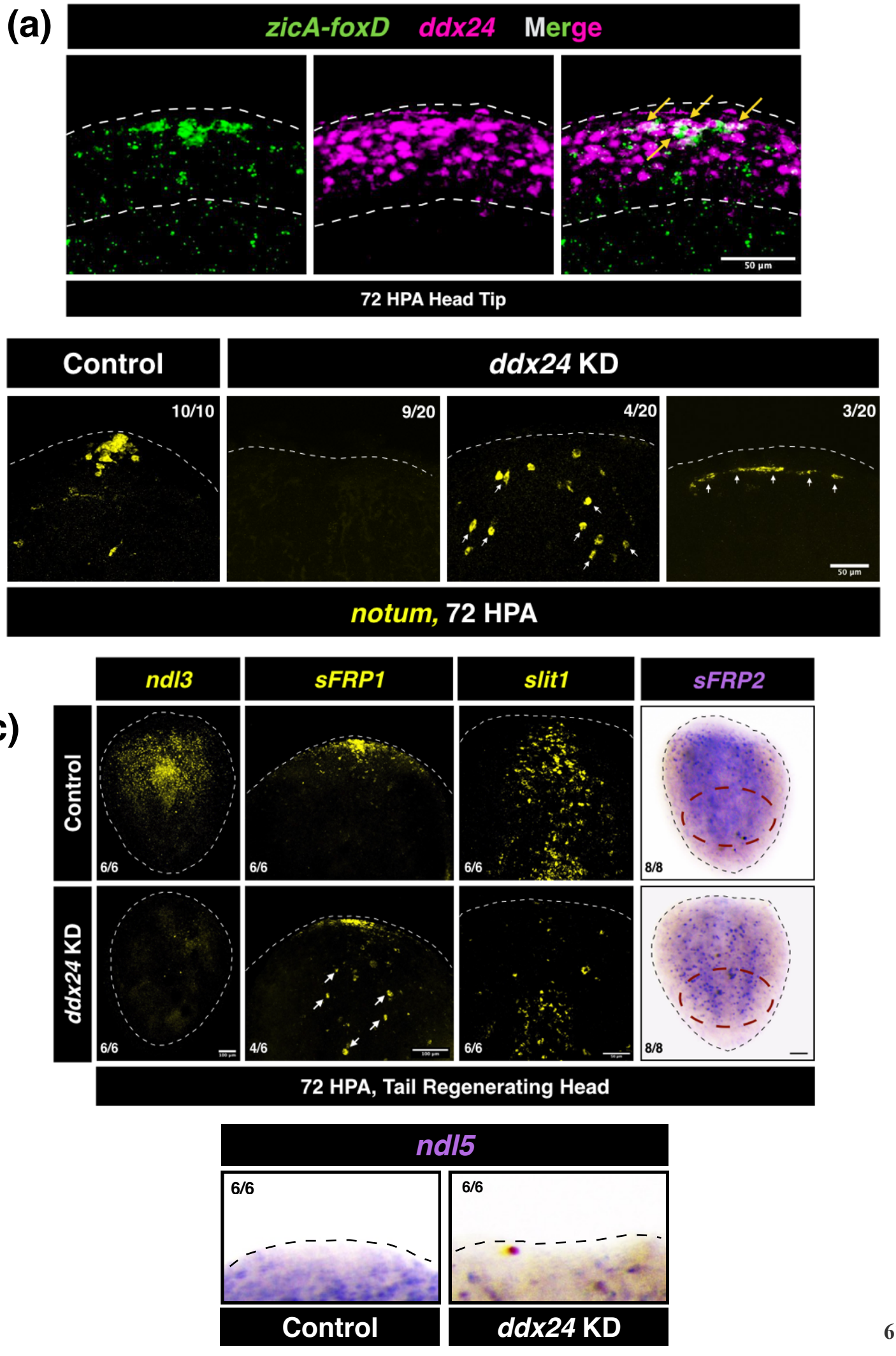

Figure 5 (Supplementary)